

University of New Mexico

## UNM Digital Repository

---

Mechanical Engineering ETDs

Engineering ETDs

---

Summer 8-1-2022

### Augmented Reality for Human Control of Engineering Tasks

Elijah Wyckoff

*University of New Mexico*

Follow this and additional works at: [https://digitalrepository.unm.edu/me\\_etds](https://digitalrepository.unm.edu/me_etds)



Part of the [Mechanical Engineering Commons](#)

---

#### Recommended Citation

Wyckoff, Elijah. "Augmented Reality for Human Control of Engineering Tasks." (2022).

[https://digitalrepository.unm.edu/me\\_etds/216](https://digitalrepository.unm.edu/me_etds/216)

This Thesis is brought to you for free and open access by the Engineering ETDs at UNM Digital Repository. It has been accepted for inclusion in Mechanical Engineering ETDs by an authorized administrator of UNM Digital Repository. For more information, please contact [disc@unm.edu](mailto:disc@unm.edu).

Elijah Wyckoff

*Candidate*

---

Mechanical Engineering

*Department*

---

This thesis is approved, and it is acceptable in quality and form for publication:

*Approved by the Thesis Committee:*

Dr. Fernando Moreu, Chairperson

---

Dr. Claus Danielson

---

Dr. Rafael Fierro

---

**AUGMENTED REALITY FOR HUMAN  
CONTROL OF ENGINEERING TASKS**

**by**

**ELIJAH WYCKOFF**

**BACHELOR'S DEGREE IN MECHANICAL ENGINEERING  
ARIZONA STATE UNIVERSITY**

**THESIS**

Submitted in Partial Fulfillment of the  
Requirements for the Degree of

**Master of Science  
Mechanical Engineering**

The University of New Mexico  
Albuquerque, New Mexico

**December 2022**

## **DEDICATION**

To my parents Christine and Edward Wyckoff, my grandfather James Ney, and my late grandmother Pauline.

To my friends and mentors for their support.

## ACKNOWLEDGEMENTS

I would like to express the utmost gratitude for Dr. Fernando Moreu, my advisor and committee chair, for continuing to encourage me through the years of classroom teachings and the long number of months preparing for this thesis. He was the first to introduce me to research and has exceeded all expectations as a mentor and advisor. He has helped me not only in my career but in my life as well.

I would also like to thank my committee members, Dr. Danielson and Dr. Fierro, for their time in not only my defense but also throughout my research, their feedback has been invaluable. I would also like to thank Dr. Petersen for his willingness to contribute and appreciate his constant support and effective feedback.

My MS Thesis was funded with support from the New Mexico Space Grant Consortium, Air Force Research labs, Transportation Research Board, Federal Railway Administration, and the US Department of Energy.

I am also extremely grateful for Marlan Ball and Jack Hanson for their help in this specific research area, without them I would not have learned and improved as much as I have. I am also thankful for Dilendra Maharjan and Dr. Justin T. Baca who were early mentors to me when I was first introduced to research. I would like to thank 2nd Lt. Joshua Murillo for his encouragement, and extend special thanks to my colleagues Maimuna, Eric, Odey, Ali, Mahsa, Kaveh, Timothy, Saiqa, Xinxing, Roya and Jiaqi and anyone else I have had the privilege of meeting through this journey.

# AUGMENTED REALITY FOR HUMAN CONTROL OF ENGINEERING TASKS

by

Elijah Wyckoff

B.S., Mechanical Engineering, Arizona State University, 2020  
M.S., Mechanical Engineering, University of New Mexico, 2022

## **ABSTRACT**

This research is motivated by the study of dynamics, especially in experimentation and Structural Health Monitoring (SHM) methods. It is important that inspectors maintain awareness of test structures while observing sensor data and inputting control. Humans receive a large amount of information from vision, and this feedback is crucial to inform decision making. Human-computer interaction (HCI) provides valuable data and information but separates the human from reality as it is necessary to look away from the region of interest to view information on a separate device. Additionally, sensor data does not collect experiment safety, quality, and other contextual information of critical value to the operator. Safety, informed decisions, and control by engineers in the laboratory or field would be increased if they could maintain focus on their environment while evaluating the data their senses are not equipped to obtain (i.e., sensors and processing equipment). Furthermore, humans could advance robotic and machine manipulation if informed on real-time of the consequences of their decisions during human manipulation. To solve this problem, this research provides humans with Augmented Reality (AR) tools for engineering tasks. AR provides additional information to the AR user via head-mounted

device (HMD), which allows the user to operate and observe the physical space without impedance. The two primary areas of focus in AR development in this MS thesis are visualization and control, where several applications are developed for specific use in engineering tasks. Elements of visualization and control are present in each of the applications. The primary application provides an interface for sensor feedback in AR. This inspires an AR interface for control of actuators in vibratory experimentation. The application is developed to plot sensor data in an interface complete with voltage, frequency, and duration controls for vibration generation. Implementing robots into cyber-physical systems for SHM promotes human capabilities that are improved by robot capabilities. Intuition often allows human workers to solve different tasks faster than robots, and when these human capabilities are coupled with the repeatability and endurance of robots then full potential can be realized. Two applications are developed for feedback and control of robotic arms in AR for the purpose of sensor deployment. The two arms are the Cyton Alpha 7-degree-of-freedom (DOF) arm and the Kinova Gen3 7DOF arm. This MS thesis also presents an AR application for an acoustic SHM method, deemed tap testing, which is used to detect signs of deterioration in structural surfaces through nondestructive means. The system is setup on a mobile robot titled Brutus, which is equipped with a sonar sensor to measure the distance between the robot and test surface. Experiments are conducted for verification of the developed applications, and the results of the reported experiments indicate that augmenting the information collected from sensors in real-time along with interfaces for control narrows the operator's focus for more efficient and informed task conduction. This thesis considers the importance of human-centered framework where often experts in SHM prefer to be present to make decisions

based on their own cognition, which can be coupled artificial intelligence and automation without solely depending on it. The research solves a problem with HCI where the operator experiences gaze distraction when attempting to monitor data and dynamic events. AR provides additional information to the AR user via HMD, which allows the user to continue to operate and observe the physical space without impedance. The results enable the research community to design, program, and examine new AR applications interfacing sensor feedback and control with real structures and environments.

# Table of Contents

List of Figures .....	xii
List of Tables .....	xvi
Chapter 1. Introduction .....	1
1.1 Overview .....	1
1.2 Scope of Thesis.....	1
1.3 Outline of the Thesis.....	3
Chapter 2. Literature Review .....	6
2.1 Introduction .....	6
2.2 Sensor Technology for Structural Inspection and Monitoring .....	6
2.3 Sensor Integrated AR Tools .....	7
2.4 Control of Experimental Tasks.....	10
2.4.1 Tap testing.....	10
2.4.2 Electrodynamic exciters.....	12
2.5 Robotics and Control.....	13
2.6 Summary.....	16
Chapter 3. AR Framework for Engineering Tasks .....	17
3.1 Augmented Reality .....	17
3.2 Human Perception .....	18
3.3 Visualization.....	18

3.4 AR to Reduce Distraction.....	19
3.5 Wireless Smart Sensor Communication.....	20
3.6 Human-structure Interfaces .....	21
3.7 Structural Dynamics Experimentation.....	23
3.8 Developed Applications .....	24
Chapter 4. Development of AR-sensor Communication and Display.....	26
4.1 Hardware for AR-sensor application.....	26
4.2 Software Development .....	29
4.3 Results of AR-sensor Development .....	32
4.3.1 Experimental setup.....	33
4.3.2 Eye tracking results.....	34
4.3.3 Synchronization results.....	37
4.4 Summary.....	42
Chapter 5. Control in Experimental Dynamics and Robotics.....	43
5.1 Methodology of AR Application for Shaker Control.....	43
5.1.1 Hardware components of shaker control application.....	43
5.1.2 Software components of shaker control application.....	44
5.2 Methodology of AR Application for Pick-and-place Control.....	46
5.2.1 Hardware components of pick-and-place application.....	47
5.2.2 Software components of pick-and-place application.....	48

5.3 Methodology of AR Application for Gen3 Robotic Arm Control .....	49
5.3.1 Interface menu and functions – position control of robot.....	53
5.3.2 Interface menu and functions – frequency of movement of robot.....	54
5.4 Results .....	55
5.4.1 Shaker control results.....	55
5.4.2 Pick-and-place control application validation .....	57
5.4.3 Gen3 move to target results .....	59
5.4.4 Gen3 frequency of movement results .....	63
Chapter 6. AR Tools for Robotic Ground Vehicle Tasks.....	68
6.1 Methodology of AR Application for Robotic Vehicle Tap Testing.....	68
6.1.1 Hardware components of Brutus application.....	69
6.1.2 Software components of Brutus application.....	75
6.2 Tap Testing Control Application Implementation.....	78
6.2.1 Tap testing experiment results .....	79
Chapter 7. Conclusions .....	82
7.1 AR for Engineering Tasks Conclusions .....	82
7.2 Recommendations .....	84
7.3 Publications .....	85
a. Journal Publications .....	85
b. Conference Proceedings.....	85

c. Book Chapters .....	86
d. Technical Reports .....	86
e. Magazine Articles .....	86
References.....	87

## List of Figures

Figure 1. Framework for wireless sensor deployment (Yang et al., 2019).....	7
Figure 2. Displacement data in AR (Aguero et al., 2020). .....	8
Figure 3. View of area measurement in AR (Ballor et a., 2019). .....	8
Figure 4. AR for annotations in an SHM application (Napolitano et al., 2021). .....	10
Figure 5. Point cloud data visualization of rockfall (Zoumpikas et al., 2021). .....	11
Figure 6. Collection of data for SHM with aerial drone (Nasimi et al., 2022).....	12
Figure 7. Human-robot interface in AR (Rosen et al., 2019). .....	14
Figure 8. AR application for ground robot guidance (Chacko et al., 2020). .....	14
Figure 9. Digital twin and robot control in AR (Manring et al., 2020). .....	15
Figure 10. Microsoft HoloLens2.....	17
Figure 11. Model of central vision in human perception (Loschky et al., 2017). .....	18
Figure 12. Current model.....	21
Figure 13. Proposed model. ....	21
Figure 14. Development flowchart for AR. ....	18
Figure 15. Framework for AR implementation in SHM.....	22
Figure 16. (a) Side view of researcher’s gaze while monitoring vibrations; (b) View from behind researcher demonstrating obstruction by screen displaying data. ....	23

Figure 17. Components of the LEWIS5 sensor. (a) Metro M4 Express; (b) MMA8451 Accelerometer; (c) Airlift WiFi Shield. ....	29
Figure 18. LEWIS5 sensor full assembly. ....	29
Figure 19. Interface menu and graph. ....	31
Figure 20. Experimental setup and eye tracking example AR and shaker-sensor. ....	34
Figure 21. (a) Eye tracking results strictly monitoring the sensor; (b) Eye tracking results monitoring sensor data plotted on separate screen; (c) Eye tracking results with AR plot. ....	36
Figure 22. Time history of each experiment. ....	38
Figure 23. PSD of each experiment. ....	39
Figure 24. Results of time offset in user’s attempt to follow moving sensor. ....	40
Figure 25. Results of user synchronization with moving sensor. ....	41
Figure 26. Results of user consistency in amplitude for the 10 excitations. ....	41
Figure 27. SmartShaker configurations (a) Shaker with stinger for sensor mounting; (b) Sensor connected to shaker to send input. ....	44
Figure 28. Shaker control interface in Unity and HoloLens view. ....	45
Figure 29. Cyton Alpha hardware. ....	48
Figure 30. Cyton Alpha control interface. ....	49
Figure 31. Kinova Gen3 robot holding a LEWIS sensor. ....	50

Figure 32. (a) Initial goal of reaching a target with robot position control application; (b) Flowchart of robot position control application development.....	51
Figure 33. Demonstration of frequency actuation by human observation.....	53
Figure 34. Position control application demonstrated in Unity and deployed in HL2. ....	54
Figure 35. Components of robot frequency control as seen in HL2 view. ....	54
Figure 36. Video frame taken after input received by shaker from HL2.....	55
Figure 37. Experimental results of exciter control without AR.....	56
Figure 38. Experimental results of exciter control with AR. ....	56
Figure 39. Flowchart of application operation.....	58
Figure 40. Movement of 3D printed object first and second position. ....	58
Figure 41. The robot with sensor approaching the target line. ....	59
Figure 42. Control results for first session.....	60
Figure 43. Time history of Test 1. ....	61
Figure 44. Time history of Test 2. ....	61
Figure 45. Time histories Test 3-5.....	62
Figure 46. Control results for second session. ....	62
Figure 47. Experimental setup and user view of experiment.....	64
Figure 48. Results of frequency response experiment. ....	65
Figure 49. Results of robot movement at frequency.....	66
Figure 50. Rockfall danger to infrastructure and civilians. ....	69
Figure 51. Brutus construction.....	71

Figure 52. Full Brutus assembly including the sonar sensor. ....	73
Figure 53. Sonar sensor components. ....	74
Figure 54. Initial goal for application development.....	76
Figure 55. Application components; (a) Drive hologram; (b) Tap hologram; (c) Steer hologram; (d) Sonar reading; (e) Eye tracking menu. ....	77
Figure 56. Example of view in HoloLens. ....	77
Figure 57. (a) Rockface location; (b) Position 1 location; (c) Brutus control view in HL2. ....	78
Figure 58. Eye gaze results for Brutus test. ....	79

## List of Tables

Table 1. HoloLens 2 relevant features (Microsoft, 2022).....	27
Table 2. Sensor breakdown.....	28
Table 3. Frequency test results.....	64
Table 4. Brutus component breakdown. ....	72
Table 5. Experimental results for operator safety and ease of control.....	80

# **Chapter 1. Introduction**

## **1.1 Overview**

In recent years Augmented Reality (AR) has drawn increased interest from areas including healthcare, education, robotics, structural health monitoring, and other engineering-related areas for its ability to blend virtual elements with the real-world environment. AR development with application to human-structure interfaces began in the 1990s. Early AR systems were used to find the location of rebars inside structures and overlaid 3D frames during construction (Webster et al., 1996). This application to infrastructure engineering demonstrates one area of interest related to engineering and AR. These AR prototypes identified challenges related to the field implementation in real structures. Technical advancements in the last decade have enabled new uses of AR to enhance infrastructure projects, including simulating designed structures before their construction, providing virtual site visits, and offering effective means for online interactions (Behzadan et al., 2015). Other examples include evaluating dimensional and geometrical position of physical objects (Shin & Dunston, 2009) and cloud computing (Chi et al., 2012). These examples ranging from the 1990s to 2015 paved the road for rapid growth in recent years, where one source cites an increase in mobile AR consumers from 598 million to 802 million from 2020 to 2021 (Makarov, 2022). The same study reports expected revenue by 2025 of \$4.7 billion for AR for engineering, behind only healthcare and video games.

## **1.2 Scope of Thesis**

The author has conducted a literature review of relevant work in the area of engineering tasks specific to experimentation and testing strategies, structural monitoring and

inspection, assembly strategies, and collaborative robots. The literature review also includes a summary of AR research in the area of engineering tasks highlighting the importance of real-time feedback and visualization to aid decision making for the AR user.

The author presents the novel interface developed for engineering applications both in the field and in the lab. The software and hardware components for AR development are also described in the thesis. The body of work includes development of AR framework with live sensor feedback and database communication. One component is developed to plot acceleration data in real-time, which is incorporated into several of the additional AR applications. This component is first implemented to inform the user for dynamic experimentation with control of electrodynamic exciters. The second implements the live acceleration plot to inform the user of sensor movement while the frequency of movement is calculated. This movement may be generated by the user themselves by holding and moving the sensor, where it is desired to estimate structural movement without having to deploy a sensor to the structure itself. This value is applied so that the Gen3 arm can match the frequency of the sensor movement for applications such as offsetting a dynamic base. The target position for sensor placement is also included as an AR capability for the Gen3. As first-step development in this area an application is built that provides the AR user with an interface to run pick-and-place sequences with the Cyton Alpha arm. An application is also developed to control a ground vehicle that is deployed to test rock fixtures to detect potential hazards, where AR provides feedback from a sonar sensor as well to inform the human's control decisions. The sections describing specific applications are separated but are related to the category of engineering tasks specifically in structural health monitoring (SHM).

Finally, the last chapter provides the conclusions of all the contributions of this research work. The author provides prevalent limitations of this proposed technology and recommends future work to overcome these barriers to implementation.

### **1.3 Outline of the Thesis**

This section describes the content of the thesis. Chapter 1 is a general introduction of the thesis work including motivation behind the work and the overview of the thesis. The outline of the thesis is described in detail, and the scope of the thesis is also provided which explains the work included in the thesis and the motivation behind this research.

Chapter 2 provides a literature review of relevant work done in the area of engineering applications specific to experimentation and testing strategies, structural monitoring and inspection, assembly strategies, and collaborative robots, which are the main areas of focus for AR development in this thesis. These include smart sensor implementation, sensor integrated AR applications, control of actuators, and robotics. It highlights the current challenges faced in developing applications for engineering tasks and discusses potential solutions for these challenges.

Chapter 3 describes the framework of AR application development for onsite and offsite implementation. It is a general description of what AR is and how it can be used, including specific details on the motivation behind the thesis. The chapter concludes with an explanation of how AR has motivated each of the individual applications included in this thesis.

Chapter 4 describes the first application which was developed to display live sensor feedback in an AR interface. The chapter details the process of AR application

development, beginning with the hardware components associated with the preliminary study. This chapter continues with a discussion of programming in the Unity game development engine in which the author builds specific scenes to address engineering task challenges. The scene includes any information to be augmented in the user's view and the scene is deployed as an application to the Microsoft HoloLens 2 (HL2) once configured with tools for mixed reality development. Other software components are explained in detail as well, especially with regards to Arduino programming associated with the sensors used in the applications. The application is described in detail in terms of the built interface and functionality, and the results of the experiment to validate the application are reported.

Chapter 5 details three of the applications which are developed for control and feedback in experimentation and robotics. The first application provides an interface for sensor feedback and control of actuators in vibratory experimentation. The other two applications are developed for robotic arms. The first arm, the Cyton Alpha, runs a pick-and-place sequence where the commands are sent from AR. The second arm is the Kinova Gen3. It is sent a target position from AR and can move at a frequency generated by the human, who monitors the frequency in AR. It concludes with a summary of the applications demonstrated in the reported experiments.

Chapter 6 presents an AR application for an acoustic SHM method set up on a mobile robot titled Brutus. Brutus is equipped with a sonar sensor to measure the distance between the robot and test surface and this information is communicated in an AR interface that includes control of Brutus. Experiments are conducted for verification of each application by a remote test and a test at a rockface in eastern Albuquerque.

Chapter 7 summarizes this thesis and outlines the main outcomes of the results. The limitations of this study are considered, and several improvements are recommended to accelerate the implementation of AR technology in SHM. Publications and proceedings related to the work outlined in this thesis are also reported.

## **Chapter 2. Literature Review**

### **2.1 Introduction**

This chapter provides current and past studies human-centered areas of interest to this thesis. The author presents past work conducted to identify the critical aspects of the relationship between humans, infrastructure, robots, and other machines. Relevant work in AR technology is discussed in the context of structural monitoring and inspection as well as collaborative robots and experimentation.

### **2.2 Sensor Technology for Structural Inspection and Monitoring**

Researchers quantify the response of structures by measuring and observing vibrations. Acquiring smart sensor data in real-time enables operators to predict failures and make informed decisions on maintenance (Namuduri et al., 2020). Smart wireless sensors are low-cost and low-power and are useful for their reliability and fast deployment characteristics (Morimoto, 2013). Forming a network of wireless sensors supports the gathering of data and decision making, and these wireless sensor networks are used for monitoring and assessing structures (Zhou et al., 2021). A WSN in Torre Aquila proved the system is an effective tool for assessing the tower stability while delivering data with low loss ratios with an estimated lifetime of over one year (Ceriotti et al., 2009). Often data acquisition occurs prior to processing in wireless sensor systems for SHM, which is why researchers have explored implementing real-time wireless data acquisition on the Imote2 wireless sensor platform (Linderman et al., 2012). Researchers have also developed a vision-based tracking method to detect damage to a structural system using cameras already installed in the system (Harvey & Elisha, 2018) and an ultrasonic wireless sensor

for fatigue crack detection to aid inspection shown in Figure 1 (Yang et al., 2019). Wireless and remote sensor systems are optimal for efficient and reliable data feedback, but there remain challenges for users to see real-time data. Open challenges remain that would be beneficial to explore in human-sensor interfaces.

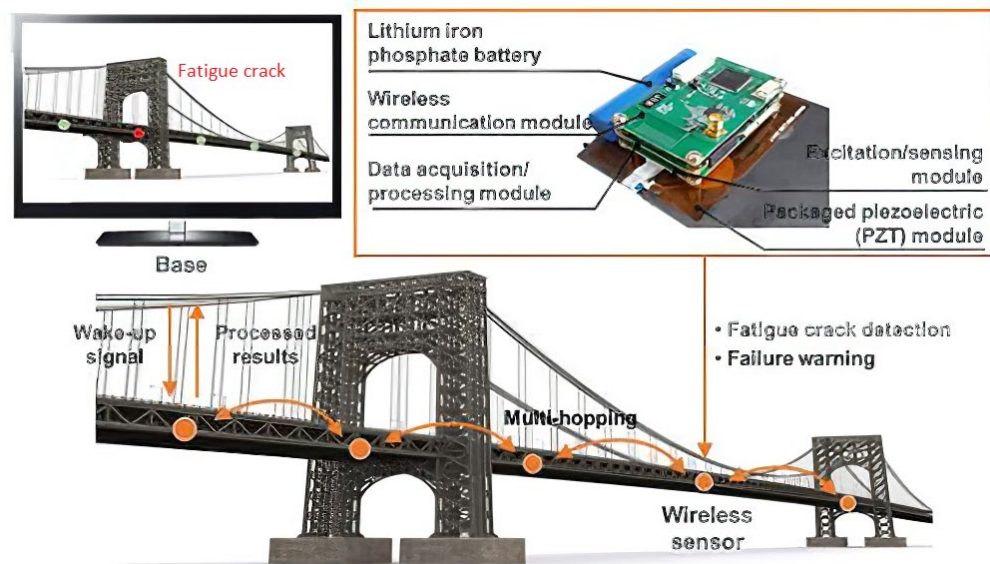


**Figure 1.** Framework for wireless sensor deployment (Yang et al., 2019).

### 2.3 Sensor Integrated AR Tools

The development of AR capabilities has strong implications for SHM. For example, AR is useful to researchers in informing of real-time data. AR has been used to augment different types of wireless sensor data including visualization of building information modeling through IoT technology (Natephra & Motamedi, 2019). Researchers have also augmented displacement data collected by smart sensors, however these values were first recorded and stored in a database before calculations were run for plotting in AR (Figure 2).

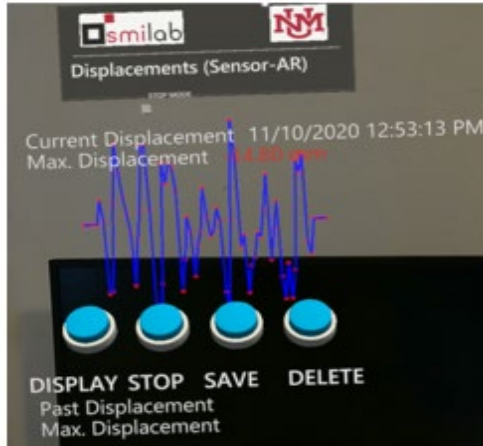


**Figure 2.** Displacement data in AR (Aguero et al., 2020).

AR in infrastructure inspections has been investigated where the framework uses the headset’s sensors to capture a high-resolution 3D measurement of the infrastructure (Figure 3). This can be used to analyze the state of the structure over time and track damage progression. Researchers have also developed a human-machine interface (HMI) which organizes metadata and provides actionable information by visualizing data about the built environment both on and off-site using AR (Figure 4).

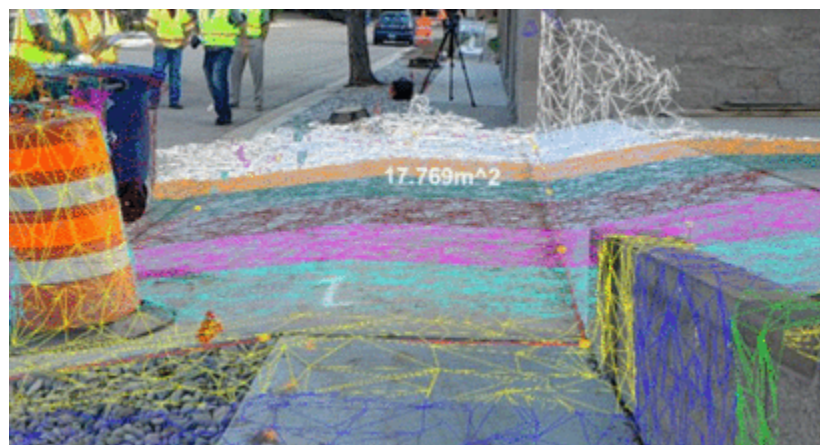


**Figure 3.** View of area measurement in AR (Ballor et a., 2019).

AR has been used for different areas of SHM including detecting heat emitted from electronic equipment (Morales Garcia et al., 2017). Wang et al. presents two AR systems

and their application scenarios for the construction industry, where this technology can be integrated into heavy construction operations and equipment management (Wang et al., 2008). AR applications are emphasized for their potential to reduce cost, time, and levels of risk by augmenting applicable events with digital content. Implementing automated driving suffers from a problem with lack of trust and user acceptance, and AR technology exists as a solution to mitigate these issues (Wintersberger et al., 2019). The prospect of increasing user acceptance and trust by communicating system decisions through AR is investigated by quantifying user acceptance using the Technology Acceptance Model. AR has been applied to manufacturing training, specifically for welding, and is also evaluated using the Technology Acceptance Model to understand how welders perceive its practicality and ease of use (Papakostas et al., 2021). Another example of AR applied to SHM is dimensional measurers, which provide inspectors with real-time quantification of distances, areas, and volumes in the field directly in their field of view without the need of physical measuring devices. Case studies performed in relatively small inspection areas show an inspector can collect dimensional information while using an AR measurer app in site at shorter time compared to conventional inspection and with the same accuracy as conventional tools (Xu et al., 2021). This includes the ability to permanently record the measurement data. AR has a wide range of uses making it a valuable tool for SHM, and this research seeks to develop a framework for the direct augmentation of sensor data and controls.



**Figure 4.** AR for annotations in an SHM application (Napolitano et al., 2021).

## 2.4 Control of Experimental Tasks

This section of literature review contains specific instances of control for experimental tasks. The first experimental task is an acoustic SHM method, deemed tap testing, which is a nondestructive means of detecting potential rockfall hazards. The second experimental task is actuating a device for vibration testing in the laboratory. Both tasks serve as motivation for AR applications developed in the scope of this thesis and are explained in further detail below.

### 2.4.1 Tap testing

Rockfall hazards pose a risk to transportation infrastructure, especially for roads and highways. According to the U.S. Geological Survey 25 to 50 people die in United States due to landslides each year (USGS, 2021). Mitigating such risks requires that engineers identify signs of structural deterioration with efficiency and accuracy, where collected information assists repair or replacement of failing transportation systems. Researchers use sensors and learning algorithms as non-contact methods of classifying damage severity in

structures (Figure 5). This aids in the evaluation of structures in the field, including estimation of the severity of damage and deterioration.

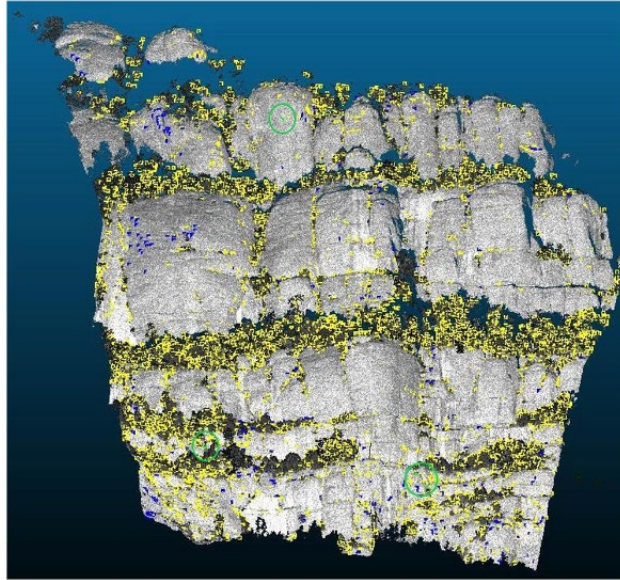


**Figure 5.** Point cloud data visualization of rockfall (Zoumpikas et al., 2021).

Data collected by sensors assist the methods of quantifying structural conditions through inspection, and robotics and cyber-physical systems can improve the process of these SHM tasks (Figure 6). Combining human cognition with the endurance and repeatability of robots ensures consistent and accurate tests while eliminating subjectivity. Additionally, safety risks can be reduced by implementing remote-controlled robots. Cyber-physical systems can be applied to transportation to increase feedback between analysis systems and the physical transportation system (Deka & Chowdhury, 2019). This research introduces the tap testing mobile ground robot without AR, which motivated the AR application developed for this specific purpose. This thesis includes one area of focus automating the classification of rock properties, informed by a tap testing device to analyze sounds collected in the field by a repeated tapping. The results of the experiment designed

to test the system show the success in the classification of the tests conducted at a rockface near a highway using the tap testing method with AR control and feedback.



**Figure 6.** Collection of data for SHM with aerial drone (Nasimi et al., 2020).

#### **2.4.2 Electrodynamic exciters**

In addition to actuating a real physical response through tap testing, actuation is required for dynamic laboratory experiments to simulate structural dynamics. Electrodynamic exciters, also known as shakers, are a common tool for generating vibrations for laboratory experimentation. Sensor failure due to mechanical vibrations and shock is tested prior to field deployment with a frame that includes three electromagnetic shakers for mechanical excitation as well as loudspeakers for acoustic excitation (Saadatzi et al., 2020). Control systems for such shakers include sinusoidal signals, adaptive algorithms, signal amplitude adjustment are examined, and a model for generating sinusoidal sweep and broadband random vibrations using an inverse filter is proposed (Čala, 2015). For this thesis, the author develops a new interface for manual control of shaker voltage and frequency with the inclusion of the live acceleration plot to fully inform the human's decisions.

## 2.5 Robotics and Control

Past work in the area of human-robot interaction (HRI) has paved the way for capabilities that are improved and enabled through AR. For example, using TCP protocol similar to that of AR applications researchers develop software to sort products using a Kinova robot arm equipped with a vision system (Prusaczyk et al., 2019). Preliminary work in virtual joystick teleoperation of 6DOF arm has been demonstrated as well (Palacios, 2015). Although the control interface does not involve mixed reality, it motivates the development that has led to AR robotic control. Physical sensors have been incorporated with robots as well for blind obstacle detection (Wisanuvej et al., 2014). Accelerometers for blind detection of obstacles and spatial mapping are implemented to avoid collision with a robotic arm, a capability that can now be applied with AR head mounted devices (HMD). Assembly strategies constantly change as product references vary and adapting the system to the changes is ineffective and time consuming from the programming point of view. AR technology is utilized to combine the benefits of existing programming methodologies with human intuition, where the presence of a human is interfaced with robotic control to adapt to changing references. In fact, Andersson et al. propose that it is possible to improve training, programming, maintenance, and process monitoring for robots with AR and investigate such methods (Andersson et al., 2016). Humans can communicate without issue, but for robot communication rely on 2D displays (Opiyo et al., 2020). This requires the human to continually pause their work to monitor robot communication. Researchers investigated efficient motion intent communication through AR for safe and collaborative work environments with co-located humans and robots (Figure 7). This is mostly a visualization tool so robots can communicate intended path in the real 3D environment,

which helps the human adjust and plan but does not offer a mode of control. Similarly, Fang et al. present a novel augmented reality-based interface to facilitate human-virtual robot interaction (Fang et al., 2014). This framework is also strictly virtual and meant for visualization and planning. Researchers have developed a novel AR spatial reference system for mobile ground robots that is suitable for novice users to provide task-specific spatial information to the robot (Figure 8). This includes placing spatial markers to allocate tasks for the robot at specific locations, where the markers may not perfectly align with the real world as placement depends solely on the user.

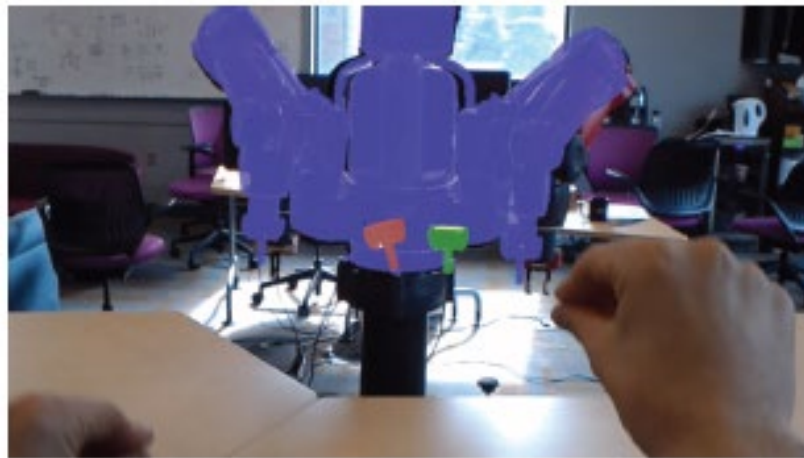


**Figure 7.** Human-robot interface in AR (Rosen et al., 2019).

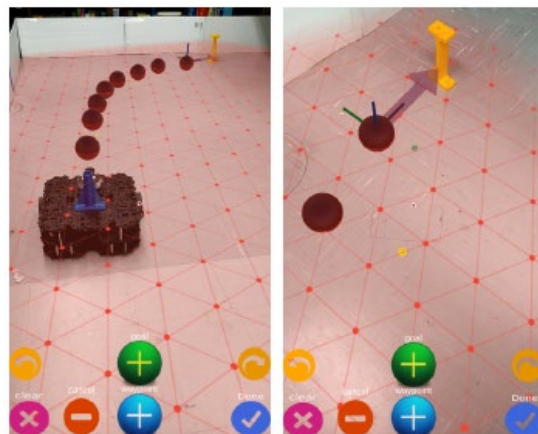


**Figure 8.** AR application for ground robot guidance (Chacko et al., 2020).

Manring et al. developed an AR application to create a more intuitive, less training-intensive means of controlling robots than traditional joystick control (Manring et al., 2020). This includes moving a holographic digital twin end effector to desired location and previewing the action of the robotic arm as demonstrated in Figure 9; however this method can be cumbersome in adjusting the digital twin correctly and has limited interaction with the real environment.



**Figure 9.** Digital twin and robot control in AR (Manring et al., 2020).

Similarly, hand tracking and manual movement of a digital twin for moving a robotic arm has been demonstrated in a project by ABB robotics (Horbst, 2020). However, the inaccuracy associated with this mode of control is not suitable for operations such as assembly or production as precise movement and placement of objects is difficult when operating this way. Researchers developed ROS Reality, a VR ROS package controlling a digital twin of the Baxter robot where the real Baxter copies the virtual twin's movement (Whitney et al., 2018). While this a relevant application of mixed reality for robot control, it still uses handheld joysticks and user does not interact with real world except through a virtual representation. In recent years interest and development of AR-related HRI has

grown exponentially, however there still exist knowledge gaps and lacking capabilities that need to be addressed.

## **2.6 Summary**

This chapter has provided the background required to explore further development into feedback and control for engineering tasks. As mentioned previously, this work focuses on visualization and control with AR. The tasks are divided into three categories, sensor feedback, control of robotics (arm sequences, remote monitoring, movement), and control for experimental tasks (shaker control, tap testing). These tasks have specific challenges which were discussed in this chapter, and the implementation of AR to address these challenges will be explained in the following chapters.

## Chapter 3. AR Framework for Engineering Tasks

### 3.1 Augmented Reality

AR incorporates virtual elements with the real-world, as this allows human users to interact with both environments. Holograms are generated by a device's computer and superimposed onto the real-world environment. For the purposes of this thesis this is enabled by a device mounted on the user's head that creates an AR environment via optical see-through display. The AR headset seen in Figure 10 is an HMD that allows for contact free operation by hand gestures and voice commands. The device is the HoloLens2 manufactured by Microsoft.



**Figure 10.** Microsoft HoloLens2.

Programming and development of AR applications is done in the Unity Game Engine utilizing the Mixed Reality Toolkit (MRTK) from Microsoft. The MRTK is applied to a scene built in the Unity application to configure the scene for AR use. The application is developed for Universal Windows Platform which allows deployment to the HoloLens 2. The programming platform is Visual Studio 2019, and the Unity scene programming is written in *C#*. These software components are organized as shown in Figure 11.



**Figure 11.** Development flowchart for AR.

### 3.2 Human Perception

Out of the five senses humans receive an estimated 80-90% of information from vision (Porter & Heppelmann, 2017). AR can reduce the cognitive load of the human by consolidating information. Understanding where this information is best perceived is important in this research, and through research the author found that central vision has the highest sharpness visually and is where humans pay the most attention to objects of interest (Younis et al., 2019). Human vision perceives a visual field of more than  $200^{\circ}$  diameter horizontally and  $125^{\circ}$  vertically, but this research is primarily interested in central vision which makes up an area of about  $13^{\circ}$  around the area of fixation (Loschky et al., 2017). Based on this information the model shown in Figure 12 is sketched.

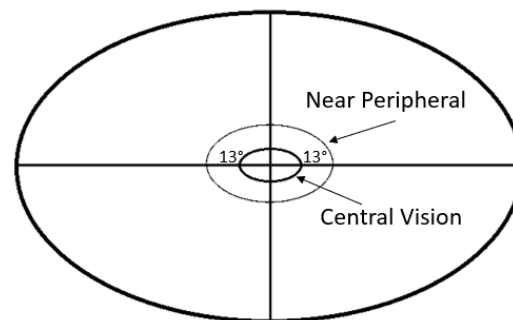


**Figure 12.** Model of central vision in human perception (Loschky et al., 2017).

### 3.3 Visualization

Visualization is a tool that is crucial to better communicate the subject matter and results. Data visualization can be useful for research in detecting outliers and trends and data

visuals are important when presenting results. When it comes to applying visuals, the circumstances under which data visualization can make a message more persuasive are defined (Pandey et al., 2014). From these circumstances they quantify the effect of data visualization in persuading test subjects to change opinions. Specific factors in visualization have been considered that have an effect on subjects' ability to understand and remember data and results. For example, color (Kim & Humphreys, 2010) and embellished visuals (Bateman et al., 2010) have been proven to significantly increase a person's memory of the results or numbers communicated through visuals. As stated previously, one of AR's primary functions is visualization. Immersive technology in education is rapidly growing in application, and AR is an example of technology that is being increasingly applied to education to help students learn with positive results (Dick, 2021). The technology is also popular in training for professionals, for example a special case of performance evaluation of AR (and Virtual Reality) technology for training EMS first responders found significant improvement in accuracy and the speed on executing tasks (Koutitas et al., 2020). Motivated by the potential of AR technology as a visualization tool to aid engineering decisions, this thesis hypothesizes that visualizing sensor data will help operators better understand structural response while reducing gaze distraction.

### **3.4 AR to Reduce Distraction**

AR technology has been applied to vehicle operation to reduce gaze distraction using AR heads-up displays to overlay images onto the windshield for navigation (Park et al., 2013). This research proves how this can reduce the mental effort of applying the information, and it prevents gaze distraction because the driver still focuses their attention on the road. AR is also applied to robot teleoperation to reduce gaze distraction, where augmenting live

video feed from the robot limits the user's view to pertinent information for safer, more controlled operation (Younis et al., 2019). Reducing gaze distraction in vibration monitoring looks to manifest safer operation and higher cognition in the same way, and gaze distraction can be quantified by measuring the area covered by a subject's eyes using the HL2.

### **3.5 Wireless Smart Sensor Communication**

Researchers interested in measuring structural vibrations are informed by the device that receives sensor feedback. If the device receiving sensor data is an AR headset, information can be relayed directly to the human (Aguero et al., 2020). With this information humans can make informed decisions that include control. This concept proposes that humans can be better informed and maintain better awareness of reality if they directly receive information on nearby structural response. Figure 13 demonstrates the current model, where the module "Gaze distraction" separates the human's awareness of reality and data. Figure 14 demonstrates the proposed model, where AR mitigates gaze distraction as a barrier to visualization and control. This research is motivated by human-in-the-loop models where it is required that human interaction is part of a control scheme. Rather than rely solely on advanced algorithms or machine learning to make decisions, this research relies on human senses and reasoning to react to changing environments. It has been reported that overlaying information from past inspections across time is a top priority for expert inspectors (Maharjan et al., 2019). It is important to fully inform humans on events such as structural movement to ensure proper decision-making occurs. In this way, humans use their intuition to solve engineering tasks with support from machines like actuators and

robots. To increase these human capabilities information must be accessed quickly and accurately.

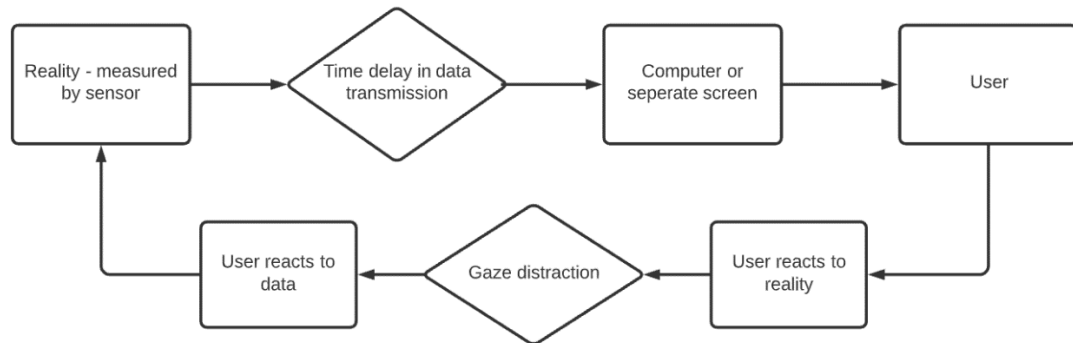


**Figure 13.** Current model.

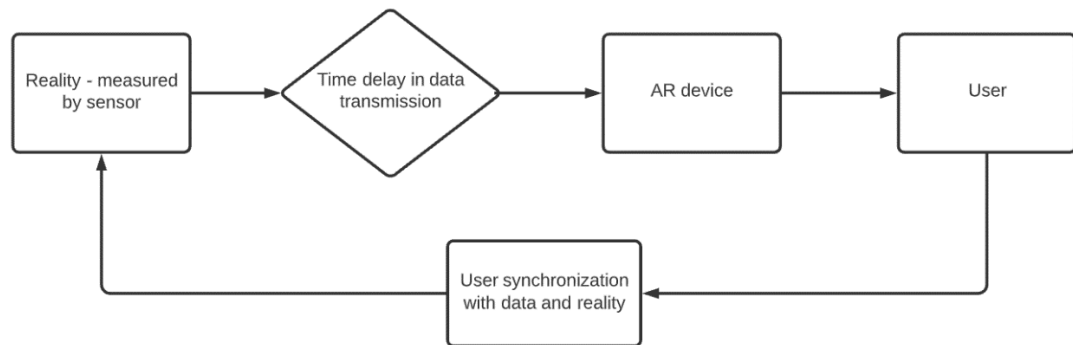


**Figure 14.** Proposed model.

### 3.6 Human-structure Interfaces

This thesis research is developed based on the concept of human-structure interfaces where the interface between human and structure informs the human on the response of the structure to enable appropriate engineering decisions, illustrated in Figure 15. For example, modes of vibration of a structure are of interest to experimenters and are typically found through finite element analysis and modelling to estimate expected behavior (Maeda et al., 2006). Augmenting sensor data allows the human to move and place sensors while maintaining awareness of the structure and the sensor location while visualizing the live

response. Therefore, AR can serve as a tool to assist an experimenter in proper sensor placement for data collection based on expected modes of vibration. This also allows the human to monitor both the structure and the data during the experiment and draw conclusions in real-time and makes it possible to ensure zero vibration at the sensor location before beginning an experiment. Additionally, wireless sensors are subject to failure when exposed to harsh conditions and other factors (Lynch & Loh, 2006). AR makes it possible to receive direct feedback on the unhindered collection of data by sensors while focusing on the structure of interest, and if the sensor were to fail the human is immediately aware. Azeem et al. tested several defects in machinery including cracks and misaligned shafts, which demonstrated significantly higher vibration amplitude (Azeem et al., 2019). This study is also motivated by detection of defects where the combination of visual feedback from the structure and sensor data in AR fully informs the human.

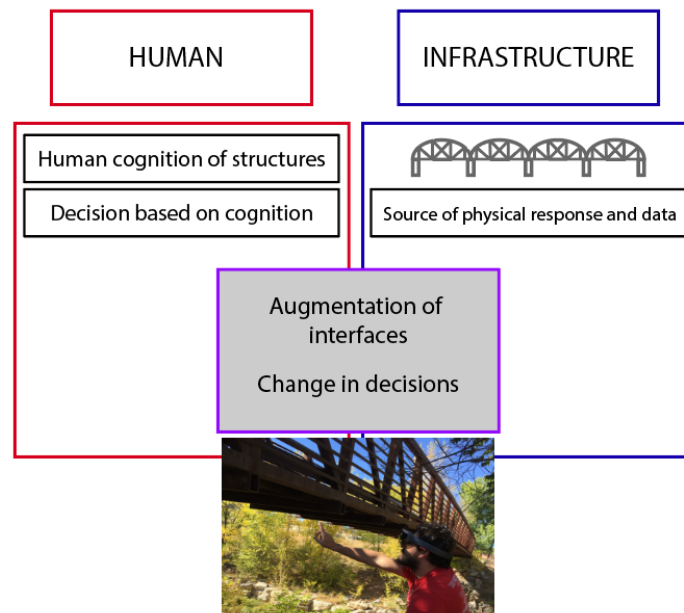


**Figure 15.** Framework for AR implementation in SHM.

### 3.7 Structural Dynamics Experimentation

The development of AR applications in this thesis is motivated by application to SHM including laboratory dynamic experimentation. Figure 16 illustrates vibration monitoring where it is necessary for the researcher to be present for experimentation. In this setup, the researcher monitors real-time vibration data collected from sensors secured to a frame. The researcher maintains focus on the suspended mass while a shaker generates excitations. Data is typically recorded and plotted on a computer screen, and the engineer tries to get the laptop as close to the structure as possible to attempt to monitor both data and the physical response. Furthermore, traditional modes of control for robotics and other machines require an application that is run on a device. Monitoring both the data, the control interface, and the structure becomes difficult when the computer screen obstructs the researcher's view. The user also depends on the location of the computer for information. This makes it difficult to make decisions based on both the data and the physical response and introduces potential issues with safety that can be addressed with AR. This motivates the two primary areas of focus in AR development in this MS thesis - visualization and control.



**Figure 16.** (a) Side view of researcher's gaze while monitoring vibrations; (b) View from behind researcher demonstrating obstruction by screen displaying data.

### **3.8 Developed Applications**

This approach to implementing AR to provide control and awareness to the user through visual feedback is utilized in three efforts in this thesis, where each implementation of AR is motivated by a human-centered approach to tasks and control. Chapter 4 introduces the first study where the author develops and tests an AR application for live feedback from a sensor collecting vibration data. This implementation of AR reduces gaze distraction in vibration monitoring and allows inspectors to monitor both the physical space and the collected data for awareness and safety.

Chapter 5 includes three of the applications which are developed for control and feedback in experimentation and robotics. The first application provides an interface for sensor feedback and control of actuators in vibratory experimentation. The application is developed to plot sensor data in an interface complete with voltage, frequency, and duration controls for vibration generation. The other two applications are developed for feedback and control of robotic arms in AR for the purpose of sensor deployment. The two arms are the Cyton Alpha 7DOF arm and the Kinova Gen3 7DOF arm. The AR interface provides control of the robot to the user where the user makes decisions based on the environment. Augmenting sensor feedback and position control provides the user with a complete interface for both perception and actuation.

Chapter 6 presents an AR application for an acoustic SHM method, deemed tap testing, which is used to detect signs of deterioration in structural surfaces through nondestructive means. The system is setup on a mobile robot titled Brutus, which is equipped with a sonar sensor to measure the distance between the robot and test surface.

Augmenting the control panel and the sensor reading fully informs the user while allowing them to maintain focus on the moving robot.

## **Chapter 4. Development of AR-sensor Communication and Display**

This research makes it possible for researchers to maintain awareness of the structures being tested while observing sensor data by building an AR interface. Normally the human's gaze shifts to a separate device or screen during the experiment for data information, missing the structure's physical response. It is important to observe real-time data, but it may distract the researcher from observing the physical response. To solve this problem, this preliminary research provides humans with real-time information about vibrations in an AR application that includes a plot of acceleration data. The application is developed to augment sensor data on top of the area of interest, which allows the user to perceive real-time changes that the data may not warn of. The thesis expands on this research by applying the concept to more applications for control with feedback from other types of sensors and devices. The results of the vibration application experiment show how AR can provide a channel for direct sensor feedback while increasing awareness of reality. In the experiment a researcher attempts to closely follow a moving sensor with their own sensor while observing the moving sensor's data with and without AR. The results of the reported experiment indicate that augmenting the information collected from sensors in real-time narrows the operator's focus to the structure of interest for more efficient and informed experimentation.

### **4.1 Hardware for AR-sensor application**

The hardware included for this section is the Microsoft HoloLens 2 headset and the 5<sup>th</sup> generation of the Low-cost Efficient Wireless Intelligent Sensor series, abbreviated as

LEWIS5. This section includes a breakdown of the HL2 features in Table 1 and describes the sensing platform developed for detecting and recording vibratory data. The sensing platform is developed to read acceleration data in a triaxial coordinate system as a wireless SHM system. The LEWIS5 sensor is built by combining a WiFi shield and microcontroller with a triaxial accelerometer. The applications that incorporate the main body of work include implementation of LEWIS5 and other versions of the LEWIS platform, which is explained in each individual section.

**Table 1.** HoloLens 2 relevant features (Microsoft, 2022).

<b>Microsoft HoloLens 2</b>	
<b>General</b>	
Field of view	52 degrees
Resolution	2k 3:2 light engines
Storage	64-GB UFS 2.1
Weight	566 g
Battery life	2-3 hours active use
Connectivity	WiFi, USB Type-C, Bluetooth
Software	Windows Holographic Operating System, Microsoft Edge, Dynamics 365, 3D Viewer
<b>Sensors</b>	
Hand tracking	4 visible light cameras
Eye tracking	2 IR cameras
Depth	1-MP time-of-flight depth sensor
IMU	Accelerometer, gyroscope, magnetometer
Camera	8-MP stills, 1080p30 video
Microphone and speakers	5 channels, spatial sound

This section provides an overview of the individual components needed to construct the sensor and includes a price breakdown to show the low-cost aspect of the sensor. A description and price point of each component is included in Table 2. The sensor connects via WiFi but requires a power source hooked up via micro-USB. The physical components are shown in Figure 17 and the fully assembled sensor is labeled in Figure 18.

## Metro M4 Express

The Metro M4 Express is a 32-bit microcontroller with the ATSAM51 microchip. The Cortex M4 core runs at 120 MHz with floating point support. The board is powered via micro-USB or barrel jack connection. The board has 25 general purpose input/output pins, including 8 analog in, two analog out, and 22 PWM outputs. The pins can collect information from sensors for use in this project. It also includes a 2 MB Quad-SPI Flash storage chip which reads and writes programs from Arduino. The board is flexible, efficient, and affordable making it a good option for this project.

**Table 2.** Sensor breakdown.

<b>Part</b>	<b>Description</b>	<b>Manufacturer</b>	<b>Price</b>
Arduino Metro M4 Express	Microcontroller	Adafruit	\$27.50
Arduino Airlift WiFi Shield	Shield + WiFi co-processor	Adafruit	\$14.95
MMA8451	Triaxial Accelerometer	Adafruit	\$7.95
Headers	Connectors	Sparkfun	\$1.50
Jump wires	Connectors	Sparkfun	\$1.95
<b>Total Cost</b>			<b>\$53.85</b>

## Airlift WiFi Shield

The Airlift WiFi Shield allows the use of the ESP32 chip as a WiFi co-processor. The Metro M4 microcontroller does not have WiFi built in, so the addition of the shield permits WiFi network connection and data transfer from websites as well as the sending of socket-based commands. The shield includes a microSD card socket used to host or store data. The shield is connected to the microcontroller with stack headers. In summary, the WiFi Shield is necessary for wireless capabilities.

## MMA8451 Accelerometer

The triple-axis accelerometer used for this project is the high-precision MMA8451 with a 14-bit Analog-to-digital converter. The accelerometer is used detect motion, tilt and basic orientation designed for use in devices like phones and tablets. For the purpose of this project the accelerometer is used to detect motion, especially vibrations. Its usage range varies from  $\pm 2G$  up to  $\pm 8G$  which ideal for its application to this project.



(a)

(b)

(c)

**Figure 17.** Components of the LEWIS5 sensor. (a) Metro M4 Express; (b) MMA8451 Accelerometer; (c) Airlift WiFi Shield.

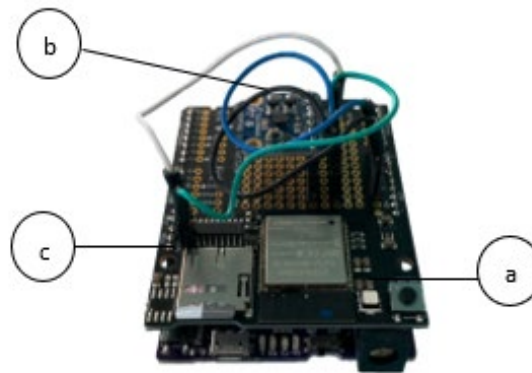


**Figure 18.** LEWIS5 sensor full assembly.

## 4.2 Software Development

The following sections explain the software components of the application, namely Arduino programming and Unity programming. Arduino programming is necessary to

configure the sensor to both record accelerometer data and act as a sever to communicate the recorded data to clients. Unity programming is necessary to develop the AR application, especially the interface which will contain all the information for the user.

## **Arduino programming**

The sensor programming was performed in the Arduino IDE, an open-source software environment that is written in Java and based on Processing and other software. This program facilitates the writing and uploading of code for any Arduino board as well as other compatible systems. A WiFi library enables the LEWIS5 sensor to be set up as a Transmission Control Protocol (TCP) server in the Arduino code. The board connects to a nearby WiFi network and accepts incoming connections on the port it is listening on. If the network is private the Arduino code includes a secret tab with the network name and password. Existing scripts for the MMA8451 accelerometer were modified to read, print, and send the acceleration data at a sampling rate of 20 points per second.

## **Unity development**

Unity Game Engine version 2018.4.19f1 was used for cross-platform development as it supports open-source programming for headsets and mobile devices. The Unity scene is configured with Microsoft's MRTK library to support the AR features of the application. The toolkit includes default scripts for necessary features in the HoloLens such as gestures, commands, and interface features. Modified code from Timur Kuzhagaliyev is implemented for connecting the HoloLens and Unity to sockets (Kuzhagaliyev, 2018). The process implements a TCP client that works for development in the Unity editor as well as for development in UWP on HoloLens. The graph of the live data is developed as a scatter

plot, which was chosen as the most effective and efficient solution. The graph is developed based on a tutorial from Catlike Coding (Flick, 2020). Points at each appropriate coordinate are generated by Unity's default cube game object, which are color coordinated based on x, y, and z acceleration. Each data point is graphed as a small 3D cube for visual feedback. The transform component is used to position each individual cube, which are variably instantiated as clones. Vector3 creates a 3D vector which defines the position of each cube. The incoming data is parsed to define each point of Vector3. At any given time there are 100 cubes generating the data lines in the display. This is defined by the resolution set in Unity, as the number of cubes is set to the value of the resolution. These cubes are connected with a LineRenderer command that makes the displayed data appear as a line chart rather than individual cubes. The graph updates with each frame meaning the cubes are adjusted as time progresses, defined by the function  $f(x, t)$ .

The first model was a bare plot of the three acceleration lines. The developed interface provides the necessary inputs for commands including client connection and disconnection and graph initiation and shut down. The full view of the interface is shown in Figure 19. The application interface consists of four different buttons with specific functionality, including Client Start and Stop and View Start and Stop.

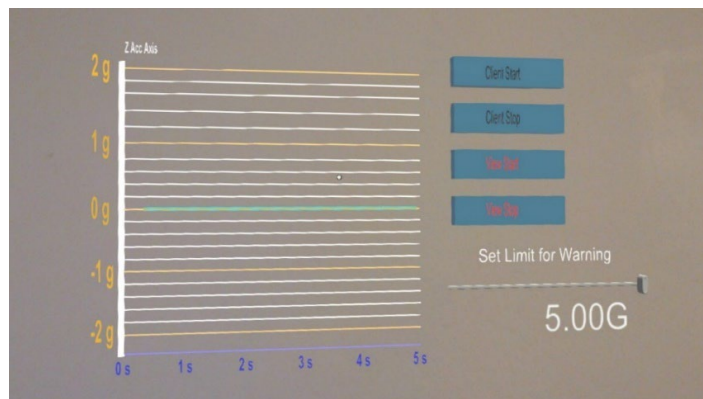


**Figure 19.** Interface menu and graph.

Client Start connects the client to the server via TCP. In the context of the application, the computer running the Arduino program acts as the server and the device running the AR application is the client. View Start button initiates the function to continue input. Incoming data from the server is parsed into x y and z vectors. Data is converted to terms of the gravitational constant G. The x and y data are also offset so that the x line does overlap and hide the y line. To verify accurate positioning of the horizontal axis lines the graph was developed using known input from an electrodynamic exciter. The x axis represents values of time in seconds that are spaced according to the sampling rate. By measuring one second intervals the x axis labels were placed accordingly. This early-stage development of an AR interface for sensor feedback is built upon as the foundation for the main work in this thesis.

### **4.3 Results of AR-sensor Development**

Researchers have examined human ability to tap their fingers at frequencies of 1, 2, and 3 Hz to investigate manual dexterity of elderly subjects (Carment et al., 2018). For this study, a researcher is tasked with following a moving sensor with a second, handheld sensor while also maintaining awareness of the data received from the moving sensor. The moving sensor is run at 1, 1.5, 2, 2.5, and 3 Hz. The objective of the experiment is to measure the level of gaze distraction while monitoring and attempting to recreate vibration data with and without AR, where it is hypothesized that human has a better sense of reality when the data is augmented in their central vision. To quantify the consequence of consolidating information to the user's central vision compared to the case of data plotted on a separate screen, an experiment is conducted to test a human's ability to monitor both reality and data while attempting to synchronize with a moving sensor. Quantifying the area covered

by the user's eyes and the user's ability to follow a moving sensor provides a means of understanding the value of AR as a tool for data visualization and control.

### **4.3.1 Experimental setup**

The experiment is designed as a first-step investigation as a new way of investigating dynamics and control. The experiment is designed to test only one subject for three different scenarios at three frequencies each for a total of nine tests. In order to remove the bias of the variability of human responses the experiment is designed to represent multiple subjects through multiple experiments to contribute to the weakness of having only one subject. The results show that the variability did not affect the results. In the future the implementation of multiple subjects will be extremely valuable for the study. Due to the subject's direct involvement in the study, the influence of implicit bias was also considered and sincerely checked to ensure it did not affect the outcome. The subject is expected to produce valuable results as based on intrinsic motivation, where the subject is more engaged by the need to gain knowledge through the experiment. This experiment serves as a first-step investigation based on a new direction in dynamics and control and provides framework for future work involving multiple subjects.

The experiment was set up with two laptop computers, two LEWIS5 sensors, a shaker, and the Microsoft HoloLens 2. One laptop computer provided power to the shaker sensor and the other laptop computer supplied power to the handheld sensor. The shaker sensor, the first laptop, and the HoloLens are connected to the network to send data from sensor to HoloLens and from HoloLens to MySQL database. The second laptop was also used to plot sensor data when measuring gaze distraction without AR. The researcher acting as the subject was positioned standing one meter from the sensor-shaker setup. The

shaker was run at 1, 1.5, 2, 2.5, and 3 Hz where a second researcher and the subject synchronize the sensors with a vertical excitation. The researcher acting as the subject begins following the shaker sensor at their discretion for a period of approximately 12 seconds. They were also instructed to maintain awareness of the data while following the moving sensor. This generates a sinusoidal plot which can be compared to the plot of the shaker sensor data to obtain time delay. Additionally, the data can be analyzed in the frequency domain to determine how well the user was able to synchronize with the shaker sensor. This data is collected using the HoloLens 2 eye tracking API, which from a target of one meter can be plotted in terms of x and y coordinates with an accuracy of 1.56 cm (Kapp et al., 2021). The user must click a button in the application UI to begin eye tracking, thus the points at the beginning and end are removed during analysis. All analysis and plot generation are done in MATLAB. Figure 20 shows the experimental setup with plotted eye tracking and the MATLAB results of the human's eye movement.

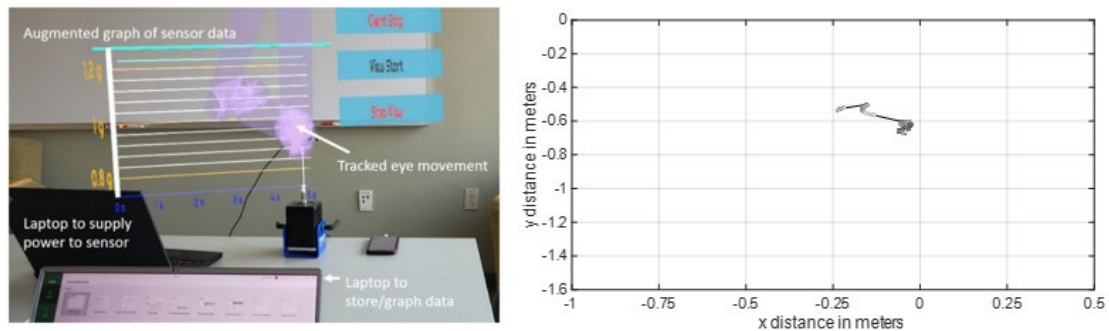


**Figure 20.** Experimental setup and eye tracking example AR and shaker-sensor.

### 4.3.2 Eye tracking results

The eye tracking data is sent from the HoloLens to a MySQL database, which is then exported as a JSON file and converted to a string and parsed in MATLAB so that the data can be plotted. The start and end points are removed by reducing the range of the data.

Each point has a three-dimensional coordinate, but this research is concerned only with the vertical and horizontal position of the eye movement. The string of data can then be graphed in MATLAB where each point is plotted and connected with a solid line representing the path of eye movement. The approximated sampling rate for the five experiments was 34. Eye tracking points for three experiments at 1.5 Hz are collected to demonstrate the importance of gaze distraction. Researchers conducted the same experiment at the three scenarios and collected the eye tracking points for approximately 50 oscillations. The time varied between 30 and 40 seconds depending on the experiment. Figure 21(a) shows the results from the eye tracking while the human is trying to match the data by observing the experiment without any dataset. Figure 21(b) shows the MATLAB results from the eye tracking while the human is trying to match the moving sensor by observing the experiment while data is plotted on a laptop screen. The figure shows that eye tracking covers the space in between the screen and the moving sensor as the human attempts to maintain awareness of both. This depends on the positioning of the monitor, so results vary depending on the experimental setup. Figure 21(c) shows the results from the eye tracking while the human is trying to match the moving sensor while monitoring data in AR. The results show that the area of eye tracking is extremely concentrated with only one diagonal observed where the human's eyes drifted to the left side of the augmented plot. The eye tracking data is heavily concentrated because the hologram of the plotted data is augmented directly on top of the moving sensor.

As expected, the eye tracking results shown in Figures 21 prove the inspector covers an area much closer to central vision than when monitoring data on a separate screen. These results help quantify the reduction in gaze distraction when monitoring an

augmented graph of sensor data rather than a separate screen. The eyes drift 0.24 m from the primary area of focus (the shaker sensor) as opposed to covering 0.97 m of space outside of central vision when checking a separate screen. The value lies in the results obtained with AR as the graph can be augmented directly on top of the area of interest. To quantify the consequence of consolidating information to the user's central vision compared to the case of data plotted on a separate screen, an experiment is conducted to test a human's ability to monitor both reality and data while attempting to synchronize with a moving sensor.

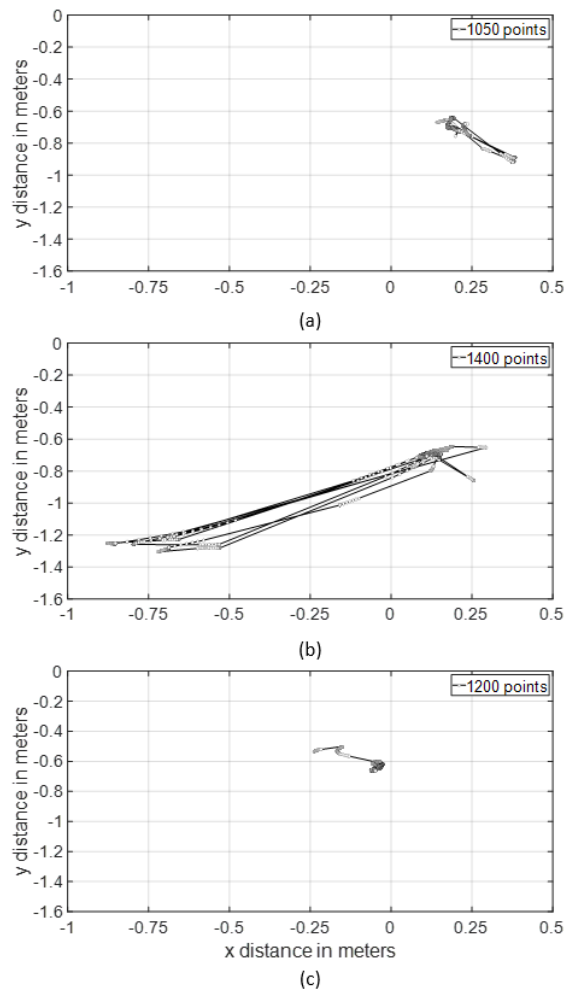


**Figure 21.** (a) Eye tracking results strictly monitoring the sensor; (b) Eye tracking results monitoring sensor data plotted on separate screen; (c) Eye tracking results with AR plot.

### 4.3.3 Synchronization results

The sinusoidal plots of the handheld sensor and the shaker sensor are plotted from the recorded data according to the sampling rate of the sensor. The time vector for the plot is generated from known values of the length of the recorded data and the sampling rate. The peak-to-peak distance between each of the first 10 shaker and human excitations is recorded manually and the average is reported as the time offset for each test as per Equation 1. The shaker plot has slight dips that indicate the point at which the shaker briefly pauses at the top and bottom of its motion, and the peaks of the human's sensor movement are clearly defined. These are the points taken as  $t_{shaker}$  and  $t_{subject}$ .

$$Time\ Delay = \frac{1}{N} \sum_{i=1}^{10} (t_{shaker} - t_{subject}) \quad (1)$$

Figure 22 shows the time history of the first 10 excitations for each experiment, where the x axis is the time duration of the 10 excitations in seconds. The plots are normalized to include the first 10 excitations for each experiment, hence the x axis labels are removed and labeled as nondimensional time. The results at 1 Hz are the clearest example of the difference between monitoring the laptop screen and monitoring data in AR. The response aided by AR closely matches the shaker, whereas the response aided by the laptop screen is significantly off for the last nine excitations. The results aided by AR also display consistent amplitude for each of the individual experiments.

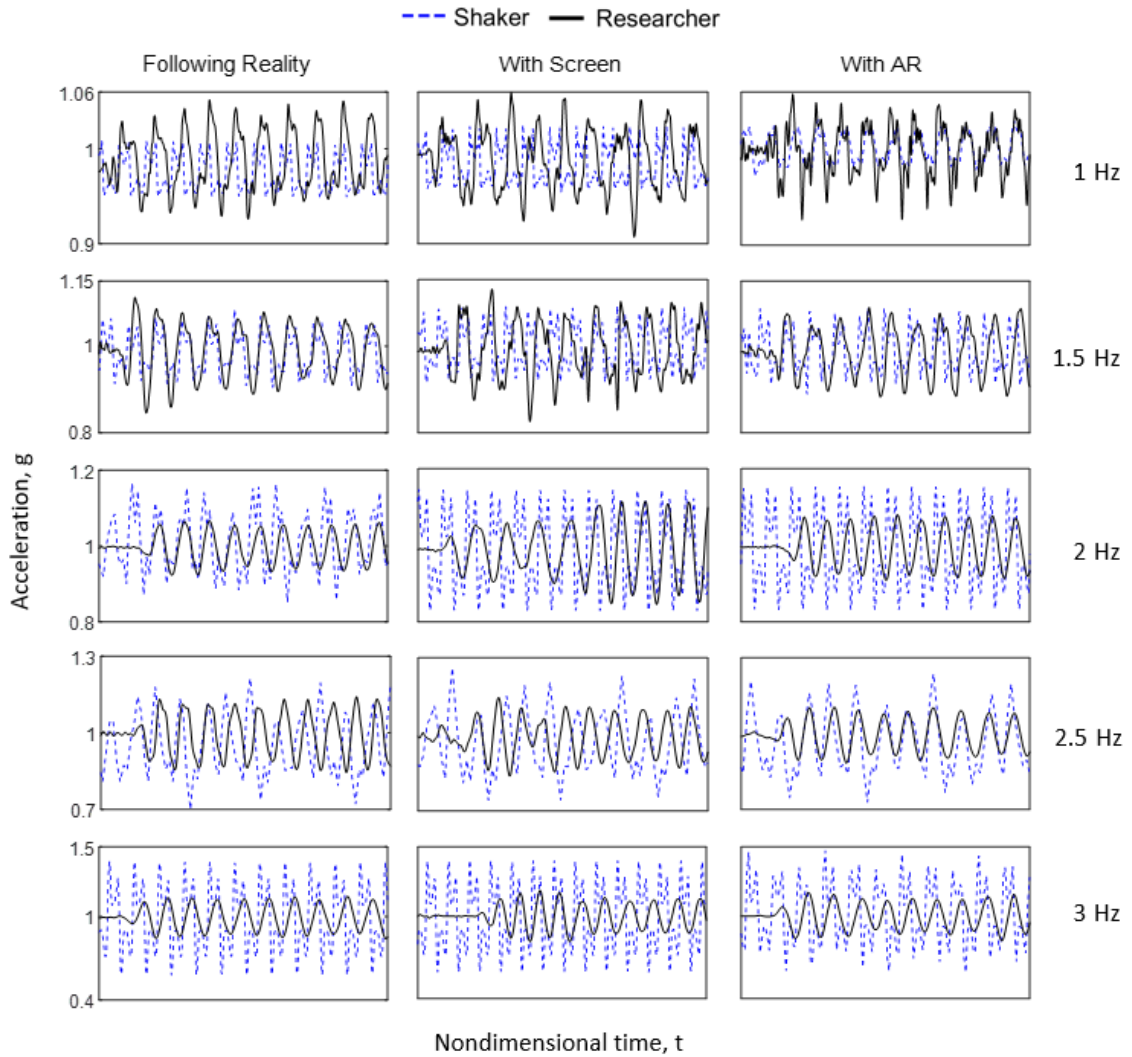


**Figure 22.** Time history of each experiment.

Figure 23 shows each individual power-spectral density (PSD) generated for the signal in relation to the frequency of the shaker, which is indicated by the vertical black line. These results are used to understand how well the human synchronized with the moving sensor. The PSD are auto-spectral density estimates generated for each single-input signal using Welch's method. This returns estimates at specified frequencies defined in the range of the sampling rate. Spikes in the PSD indicate that the signal is correlated with itself at regular periods, and thus indicate the spectra with the greatest effect (Hunter, Cross

& Nelson, 2018). This is done to determine the frequency of each signal, including that of the shaker since the shaker frequency cannot be assumed to be exact. The results for following the shaker while monitoring data on a computer screen, termed “with screen,” indicate an asynchronous result in each PSD. Conversely, the PSD results with AR show that the human was able to generate a signal with a frequency close to that of the shaker sensor.

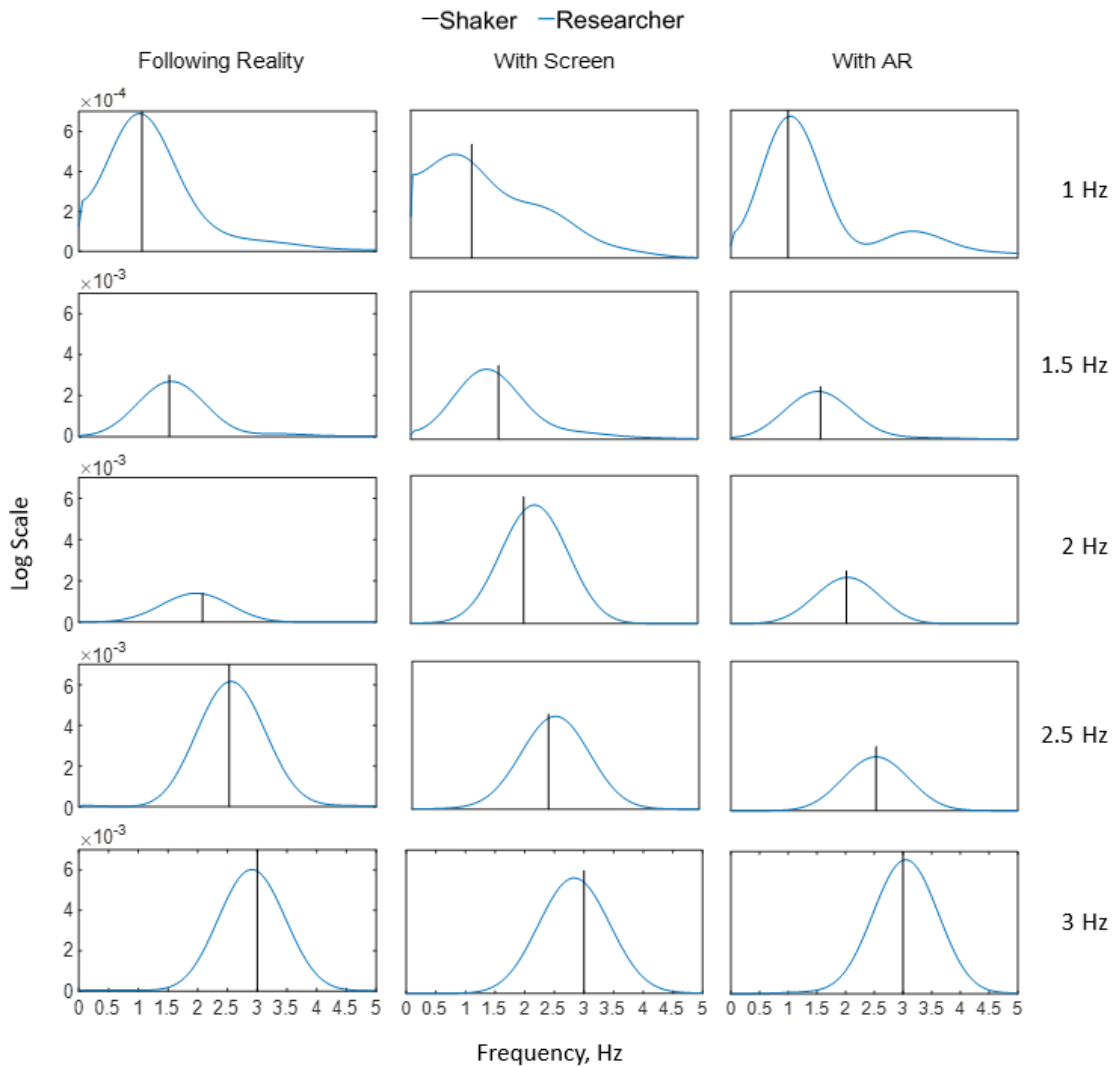


**Figure 23.** PSD of each experiment.

Figures 24-26 display bar graphs of the reported results. The results are calculated from the range in which the human attempted to follow the shaker, with the first 10 excitations considered as the range for time delay calculations. Combining the eye tracking results with the results from the handheld sensor prove increased awareness of reality while using AR. Experiments at higher frequency were considered, however the human has difficulty recreating a faster response and the results are less valuable with shorter excitations. As expected, the human performed the worst when attempting to maintain awareness of data plotted on the computer screen. Figure 24 reports the average time offset between the response generated by the human and the response from the shaker sensor. The human struggled the most at 1 and 2 Hz with the separate screen, with an average delay of 0.31 and 0.3 seconds respectively.

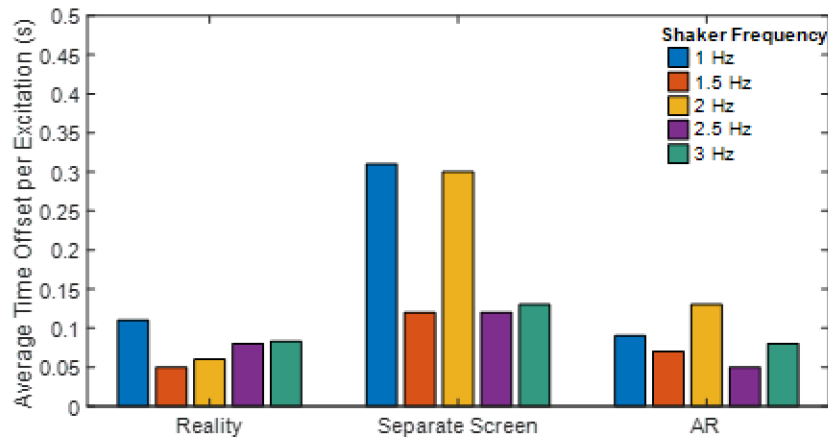


**Figure 24.** Results of time offset in user’s attempt to follow moving sensor.

Figure 25 shows the results of the human’s synchronization with the moving sensor calculated from the PSD results of Figure 23. The human created a response with significantly worse synchronization and consistency when monitoring the computer screen. Conversely, they generated a frequency with less than a 0.1 Hz offset for each of the

experiments with AR and reality. Notably, the human performed better with AR at 2 Hz than solely following reality and had very similar results at the other four frequencies.

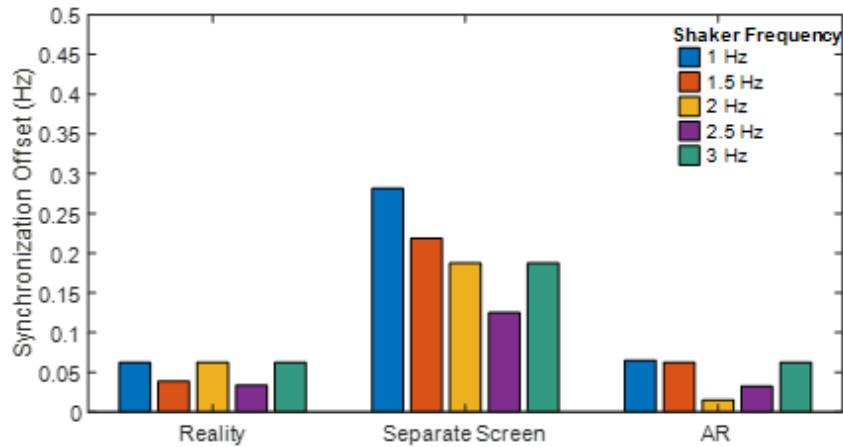


**Figure 25.** Results of user synchronization with moving sensor.

Figure 26 displays the results for the standard deviation of the 10 peaks of the signal generated by the human. The human generated consistent amplitude at 1.5 Hz compared to the other two cases, however the standard deviation of the excitation peaks for the other four experiments was much higher in comparison. The human was more consistent with AR for each experiment with similar standard deviation compared to the results with reality.

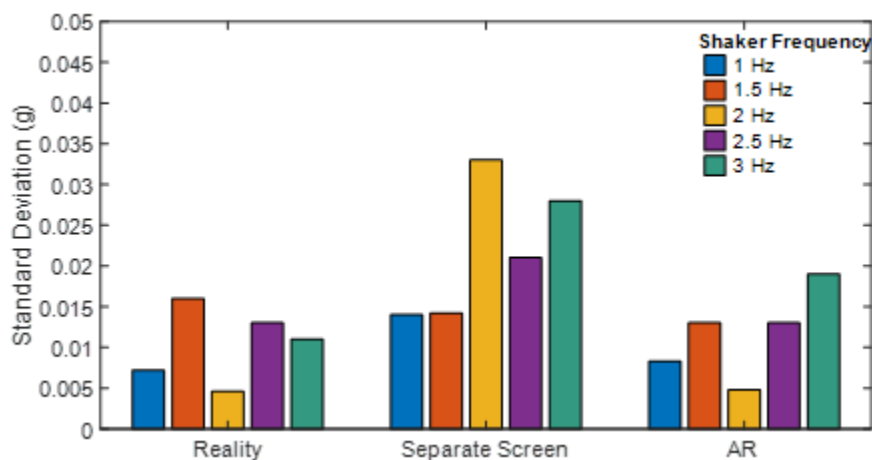


**Figure 26.** Results of user consistency in amplitude for the 10 excitations.

From the combined results for time offset, synchronization and consistency it can be concluded that AR is an improved solution in vibration monitoring. Compared to the results of the case following reality, the results with AR are consistently in a similar range. This conclusion was expected as AR provides the ability to focus on both reality and data, whereas monitoring data with a separate device does not.

#### **4.4 Summary**

This first-step study developed and tested an AR application for live sensor feedback to reduce gaze distraction in vibration monitoring. An experiment was conducted to determine if augmenting data gives a human better awareness of reality by allowing the human to remain focused on the physical space. By tracking the human's eyes, an experiment proved that gaze remains close to the primary area of focus when monitoring vibration data in AR. Additionally, the human was able to use a handheld sensor to closely replicate the response of a sensor in the primary area of focus while maintaining awareness of the vibration data. Compared to the same test with the data shown on a separate screen, the human performed significantly better which demonstrates the improved sense of reality. This implementation of AR technology for engineering reduces gaze distraction in vibration monitoring and allows inspectors to monitor both the physical space and the collected data for awareness and safety.

## **Chapter 5. Control in Experimental Dynamics and Robotics**

This chapter of the thesis work is motivated by human-machine interfaces in vibratory experimentation and robotics. HMI is crucial as it provides feedback and control interfaces for human operators to engage in. This chapter develops HMI in AR for feedback and control in engineering tasks.

### **5.1 Methodology of AR Application for Shaker Control**

This section of the thesis work is motivated by human-machine interfaces in vibratory experimentation. This application is based on a human-in-the-loop model where human interaction is necessary for experimentation. In the case of experimentation humans have a better sense of reality when aware of the real structural response and the data measured by sensors. Sensors do not inform on all events that humans are aware of by observation, and humans cannot quantify the structural response without the data from sensors. Therefore, experimenters must be aware of the real structure and the vibration data to make informed decisions, which include changing external input.

#### **5.1.1 Hardware components of shaker control application**

The LEWIS5 platform is implemented in this application. The shaker used in this research is the SmartShaker Model K2004E01 electrodynamic exciter made by the Modal Shop, the same shaker used to verify the position of the vibration plot application. The shaker is a portable permanent magnet shaker with an integrated power amplifier in its base. The excitation signal from a function generator is plugged into the BNC connector at the shaker's base. The function generator used in this research is an application that runs on a

mobile device. The exciter provides up to 7 pounds pk sine force and is supplied with a DC power supply. To validate and position of the AR graph of sensor data, the LEWIS5 sensor is mounted to the shaker by a 10-32 nylon stinger seen in Figure 27(a). By running the shaker at specified values the hologram of the graph is created at an exact position. To receive input signal from the HoloLens to the exciter, a LEWIS5 sensor connects to a 3.5mm adapter so the board can be connected to the BNC connector in the same way as the function generator device as seen in Figure 27(b).

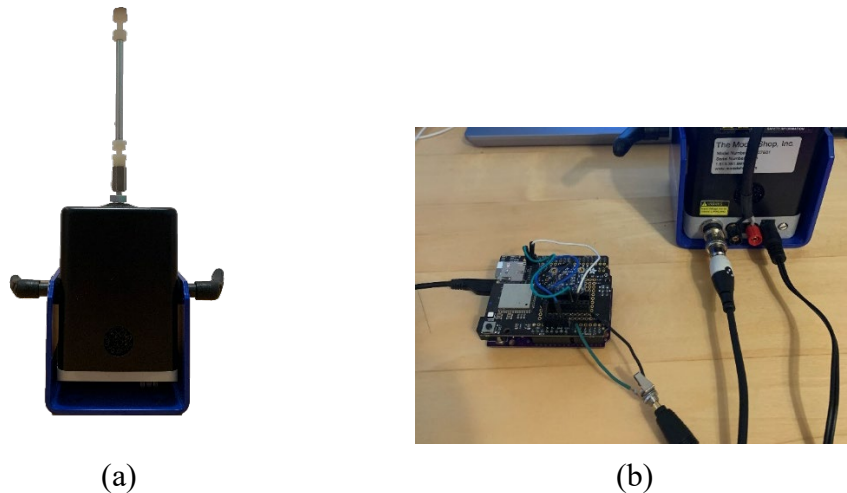


**Figure 27.** SmartShaker configurations (a) Shaker with stinger for sensor mounting; (b) Sensor connected to shaker to send input.

### 5.1.2 Software components of shaker control application

The sensor programming was also performed in the Arduino IDE. The Arduino program is written so that the sensor first connects to the WiFi whose name and password are defined in the program. As before the LEWIS5 sensor is set up as a TCP server. The board is set up as a server so it can receive messages from clients connected on the same WiFi network and port, and when receives a message from the HL2 it calculates the sine table with 256 entries at the voltage setting defined in the AR application by the user. Unity version

2018.4.19f1 was again used for cross-platform development. The Unity scene is configured with MRTK again and the vibration plot scene is imported. This project is concerned only with low-G vibrations, so the range of the graph spans 0.8-1.2 G. This meant that the graph needed to be repositioned, which was possible by the same method of attaching the sensor to the shaker.

Four sliders are created in Unity for the user to define values of voltage, frequency, value multiplier, and duration. The first slider is used to change the value of the exciter's amplitude. Changing the frequency defines the frequency of the sinusoidal signal the exciter generates. The multiplier value makes it possible for the user to increase the other values past the limit induced by the length of the slider. Finally, the fourth slider defines how long the exciter runs in seconds. The full view of the interface in both Unity and the HL2 view is shown in Figure 28. The application interface consists of four buttons for the sensor graph and four sliders for exciter input with a send button. There are buttons to connect and disconnect from the vibration sensor, and two buttons to start and stop the view of the graph as well. The sliders for exciter control include voltage, frequency, a multiplier, and seconds. The send button sends the current values to the sensor connected to the exciter.

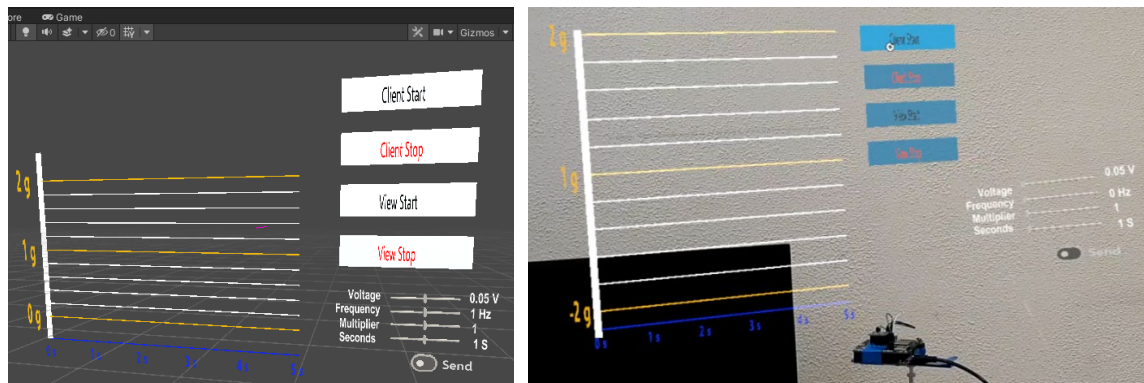


**Figure 28.** Shaker control interface in Unity and HoloLens view.

## **5.2 Methodology of AR Application for Pick-and-place Control**

Simple robot models exist as practical, low-cost instruments for flexible production. Robotics and AR research present a number of possibilities including direct manipulation of robot skills and use of low-cost hardware. This application seeks to leverage AR for a servomotor controlled robotic arm for sensor movement, placement and other pick-and-place commands for flexible production. This can be done with straightforward button selection for specific commands where code for the robot is developed in servo sequencer then defined in Arduino, similar to the original framework of sequences run through wired connection to the control box. Existing technology includes writing sequences which are stored and communicated to the robot automatically in a repeating pattern or manually by the operator, but a solution does not yet exist that combines the capabilities of AR with programming done in servo sequencing software. This project focuses on manual control of the sequence communication similar to operating a switch. Rather than communicate prewritten sequences through a computer, the commands can be communicated to the robot through the HMD which reduces gaze distraction for the human while giving them the freedom of interaction with the robot, rather than switching between separate devices. Additionally, this removes the need for a physical connection to the robot or controller. The robot control box has previously necessitated the connection of a computer to communicate servo sequences, however the implementation of LEWIS enables wireless connection to the arm. The robot itself and the control modes typically implemented in its utilization are dated, however this project seeks to advance a preexisting functional model and method of control rather than allow them to become obsolete. This method is

accessible, affordable, and intuitive as an immediate solution to flexible production requirements.

For wireless control of a robot, a connection between the control mode of a robot and the method of command must be established. In most cases, a network connection is established between a computer application and the HL2 (Hui-ping et al., 2011). This framework may not be wireless, as often it is necessary to connect the robot to the computer running the application. This is also not a viable solution for older robot models that do not have wireless capabilities, or for which control applications do not exist. We instead propose low-cost hardware that enables a connection not previously possible. This is done using a version of the LEWIS platform. The board is constructed with a WiFi shield and microcontroller. This makes it possible to interface between the control mode of the robot and an AR command hub, which is established in a head-mounted device. For this project LEWIS is implemented in one 7DOF manipulator arm (Cyton Alpha). The following sections explain the development of LEWIS with its use for wireless communication and control.

### **5.2.1 Hardware components of pick-and-place application**

The LEWIS platform is implemented for this application. The Cyton Alpha is an older model servomotor controlled 7DOF manipulator arm. For the Cyton Alpha connection the board is built just with a microcontroller (Arduino UNO) and Airlift shield. The sensor connects via WiFi but requires a power source connected via USB-B. Three pins on the board connect to the control box for the robot, which is attached to a single output switchable power supply. The hardware components can be seen in Figure 29.

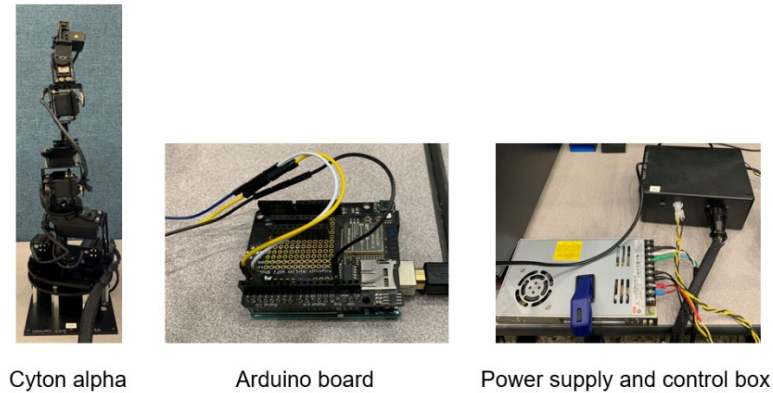


**Figure 29.** Cyton Alpha hardware.

### **5.2.2 Software components of pick-and-place application**

Servo sequencer is software commonly used for programming specified commands for older servo-driven robots. In this project sequences are written in SSC-32 servo sequencer utility by Flowbotics studio. Each servo is listed in numerical order where the value of control ranges from 500-2500. There are six joints on the arm defined as servo 1-6 where servo 7 controls the extent of the gripper's opening. The Lynxmotion recording software allows a specific sequence of servo definitions to be recorded according to the user's needs. This can then be saved as a pattern for future implementation with a robot. First, the pattern is written according to specific pick and place positions in the Cyton Alpha's nearby environment. This pattern is tested as a means of validation before the proper servo values are recorded to include in the Arduino code. Unity Game Engine version 2018.4.19f1 was used for application development. Each button in the AR interface sends a specific command to the listening Arduino board, where the command corresponds to a pre-defined sequence. This is based on two positions for pick-and-place commands where the button options include "pick" where the gripper closes on a position and "place" where the gripper opens at a position. The interface in the HL2 is displayed in Figure 30.



**Figure 30.** Cyton Alpha control interface.

### **5.3 Methodology of AR Application for Gen3 Robotic Arm Control**

As research in the field of robotics continues to grow, increasing use of AR is implemented to reduce the complexity of controlling robots. Assembly strategies constantly change as product references vary and adapting the system to the changes is costly from the programming point of view. AR technology is utilized to combine the benefits of existing programming methodologies with human intuition, where the presence of a human is interfaced with robotic control to adapt to changing references. Today, AR and VR in robotics include how different hardware and software can collaborate with human and robot system to program and handle maintenance. Satellites are commonly equipped with robot arms to perform maintenance tasks (Mitsushige, 1997). When attached to a moving structure in such cases, the arm must receive some feedback as to the dynamics of the structure to maintain balance and correctly reach a target. Rather than rely only on machine learning and other techniques, this research is interested in human-centered control where actions are based on human cognition of the situation, which can be combined with machine learning and other techniques. The author spoke to experts in the area of SHM and dynamics at Los Alamos National Laboratories (LANL) and received feedback on the

topic of human presence in situations like inspection, and the experts encouraged a human-centered approach based on their own preference of being present to make decisions based on their own expertise. This section of the thesis proposes an AR application to control the position and frequency of movement of a 7DOF robotic arm by human actuation.

### **Kinova Gen3 7DOF arm**

The Kinova Gen3 is a 7DOF robotic arm with a gripper end effector and 3D/2D vision module as shown in Figure 31. The arm has a continuous payload of 4 kg, a maximum reach of 0.902 m, consumes 36 W of power, and is described as an ultra-lightweight robot at under 8.2 kg of weight. It comes with a MATLAB support package which is integrated in this project and includes 1 kHz closed-loop control at low level with infinite rotation on all joints and smart actuators with integrated torque sensors (Kinova, 2022). Its lightweight, portability, and minimal setup time make it an ideal candidate for mobile robot implementations in engineering tasks.

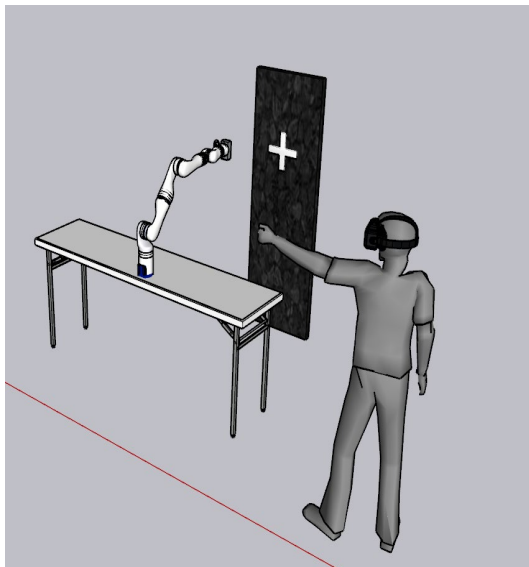


**Figure 31.** Kinova Gen3 robot holding a LEWIS sensor.

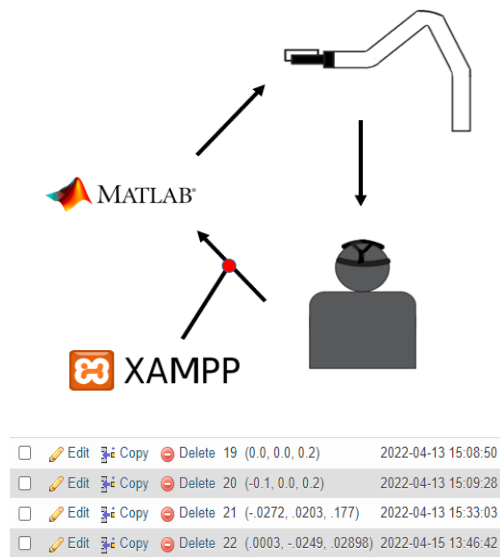
Programming and development of the AR applications is done in a newer version of Unity to apply more recent settings. Version 2019.4.10f1 is used for AR scene development and the LEWIS5 platform is again implemented for feedback. The sensor programming for the frequency component of the Gen3 components was performed in the

Arduino IDE. The board is again setup as a server so it can receive messages from clients connected on the same network and port.

The initial goal of the robot position communication application is demonstrated in Figure 32(a) where the AR user defines the origin position of the arm and a target position with two holograms. The target position is set based on the placement location that is desired by the human. This defines the robot coordinate system in the same coordinate system as the HMD. Thus, it is possible to calculate the position vector necessary for the robot to perform the desired operation. This vector is calculated by the HL2 sensors in meters in the HL2 coordinate system and is sent to a MySQL database where it is permanently stored. As demonstrated in Figure 32(b), this serves as the connection between the HL2 and the robot as MATLAB pulls the most recent position from the database and runs the code written to operate the position of the robot's end effector. The loop is closed by the user's decision making based on visual feedback of the robot's position.



(a)



(b)

**Figure 32.** (a) Initial goal of reaching a target with robot position control application; (b) Flowchart of robot position control application development.

To control the frequency of the robot movement as a means of offsetting a dynamic platform the Arduino program is written to calculate the frequency of movement along any axis of the accelerometer. This means that sensor data can be communicated to the robot to offset potentially harmful dynamics, whether through a sensor attached to the base or by human input demonstrated in Figure 33 where a human can match the movement of the base to control the frequency of the robot's movement. ArduinoFFT library is implemented as it contains a definition for fast Fourier transform in the Arduino IDE. Fast Fourier transform is an optimized algorithm for implementing the discrete Fourier transform (DFT), and the DFT is defined by Equation 2, where N is the length of the filter and  $k = 0, 1, \dots, N-1$ .

$$X_k = \sum_{n=0}^{N-1} x_n * \left[ \cos\left(\frac{2\pi kn}{N}\right) - i * \sin\left(\frac{2\pi kn}{N}\right) \right] \quad (2)$$

The code takes a defined number of samples from one direction of accelerometer data and calculates the most dominant frequency in that range using the forward FFT function with Hamming windowing. The Hamming window is given by Equation 3.

$$w(k) = 0.54 - 0.46 * \cos\left(\frac{2\pi k}{N-1}\right) \quad (3)$$

The peak value is calculated every 2.67 seconds and each new value is posted to the database. Simultaneously, the value displays in the HL2 application which is also reading from the database. The user reacts to the exact value they are generating while monitoring the signal of the handheld sensor as well. MATLAB pulls the value in the same way as the position control app. The MATLAB code defines the number of points to be covered in a span of 10 seconds based on the frequency value. The initial maximum value of frequency is defined to be 2 Hz. If the value of the calculated frequency eclipses the

maximum the code does not run. Thus, the AR component is necessary for feedback to the user of the frequency value to ensure the threshold is not crossed.

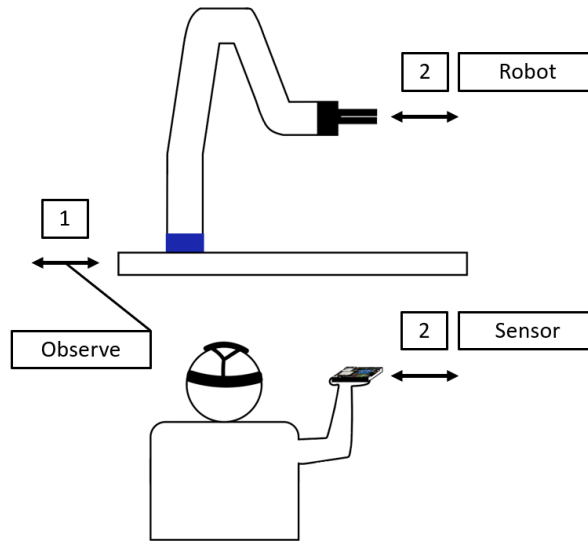


**Figure 33.** Demonstration of frequency actuation by human observation.

### **5.3.1 Interface menu and functions – position control of robot**

The full view of the interface is shown in Figure 34 where the lefthand view is Unity and the righthand view is in HL2. The interface simply consists of a send button to send the position vector between the two holograms, open and close gripper buttons, and a button to reset the robot to a rest position. As shown on the right the user moves the origin orb to the base of the robot and the target orb is set to a desired position. The application automatically connects to the database upon opening the application, so all that is necessary is selecting send to store the position. In the first version of the application the origin orb was colored green, then was changed to dark blue to match the base of the robot.

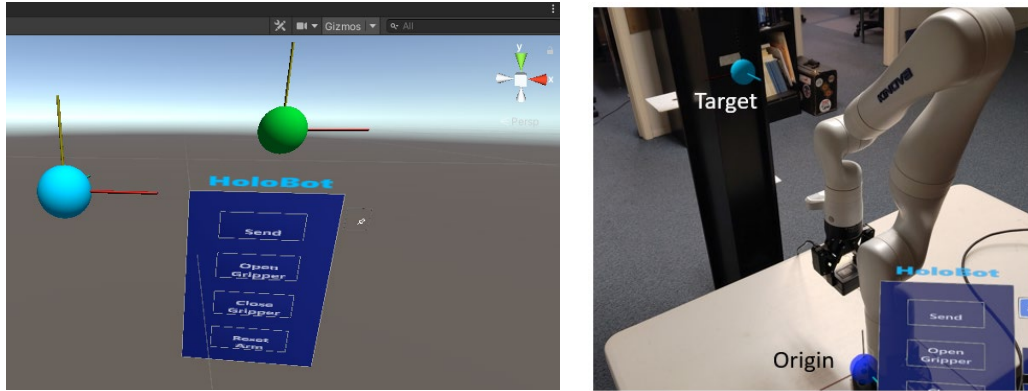


**Figure 34.** Position control application demonstrated in Unity and deployed in HL2.

### 5.3.2 Interface menu and functions – frequency of movement of robot

The full view of the interface is shown in Figure 35. The application interface consists of the plot of sensor data where the frequency of this response is updated in the bottom right corner of the graph. The same buttons from the shaker control application are included to connect to the server and begin viewing the data. The frequency, boxed in black, updates every 2.67 seconds in the user's view and this frequency depends on the movement of the handheld LEWIS5 highlighted in blue. Boxed in red is the display of the active database seen on a laptop screen which updates with each new frequency value.

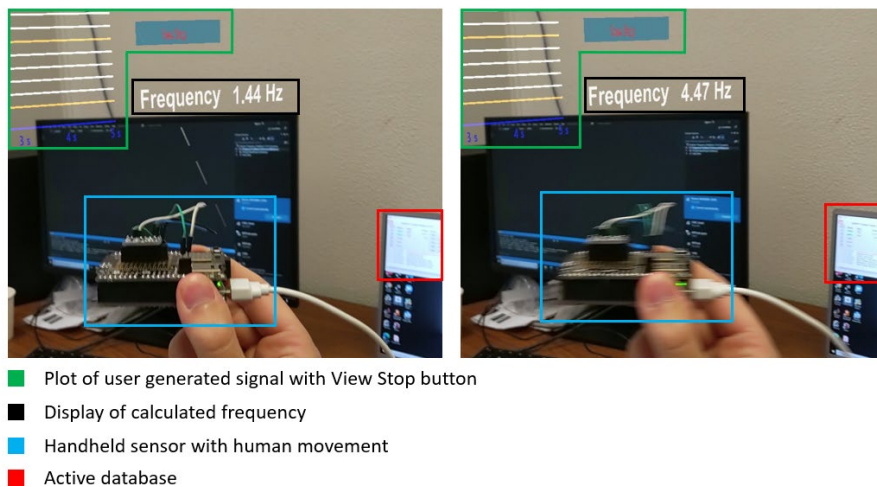


**Figure 35.** Components of robot frequency control as seen in HL2 view.

## 5.4 Results

The experiments for each application are designed to validate the applications for implementation. The shaker application tests the time delay in sending, receiving, and actuating a shaker response. The test for the Cyton Alpha investigates the repeatability of the application. The Gen3 tests are designed to test how efficient the position control application can be for novice users and the accuracy of the frequency control application.

### 5.4.1 Shaker control results

The shaker control application is tested to determine the time delay in actuation. The time delay in the program is investigated using video analysis, a frame of which is displayed in Figure 36. By calculating the frames between the initial sensor acceleration and the recorded response the time delay can be approximated. The HoloLens camera records 1080p30 video. With the known value of the video framerate in FPS the time delay of the application can be calculated using Equation 1 from Chapter 3. Frame<sub>0</sub> was designated as the time of initial acceleration by the sensor. The results were processed in MATLAB.

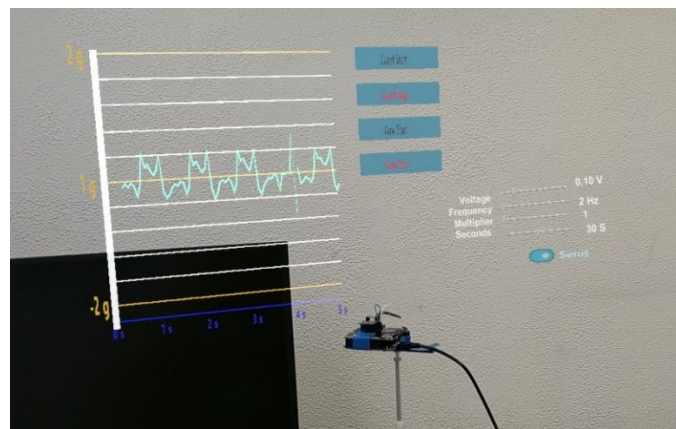


**Figure 36.** Video frame taken after input received by shaker from HL2.

Figure 37 plots the time delay in seconds recorded for each of the 14 trials conducted with the standard method of using a function generator for input to the exciter. Figure 38 shows the time delay in seconds recorded for each trial with the AR control method. The time delay with AR is an average of 0.37 seconds between the moment “send” is pressed and the exciter moves. The delay using the function generator comes out to an average of 0.20 seconds for the 14 trials. While the results show that the traditional method of control is about 0.17 seconds faster on average, this result is better than expected considering the delay introduced in a network connection. By testing the time delay in control with and without AR a quantitative comparison can be drawn between the different control methods.

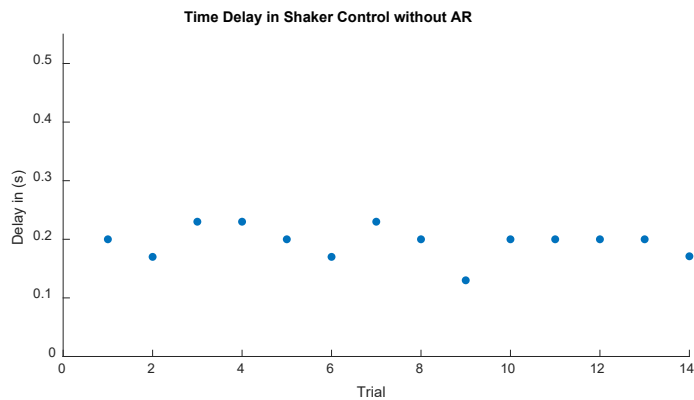


**Figure 37.** Experimental results of exciter control without AR.

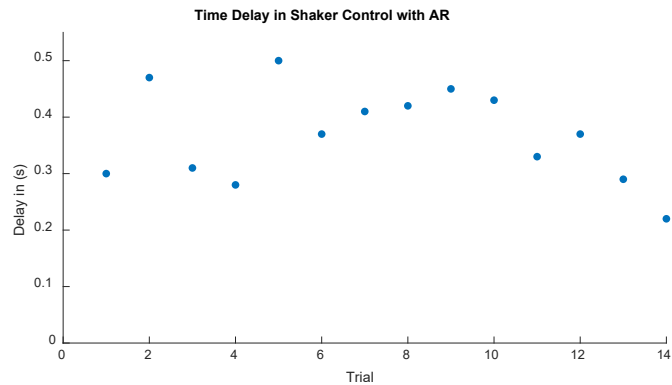


**Figure 38.** Experimental results of exciter control with AR.

This application is designed to be incorporated into vibratory experimentation based on the perceived limitations that exist in traditional modes of excitation. The incorporation of the sensor data feed into the shaker control interface fully informs the user and enables full awareness of both the physical response of structures and the measured response. The key contribution of this work can be summarized as follows:

1. This method improves cognition by allowing the operator to maintain awareness of the structure while adjusting experimental conditions, where AR effectively eliminates gaze distraction.
2. The reported experiment serves as a first-step investigation into control with AR.
3. The new shaker control loop was tested and compared it to a traditional method of using a function generator by measuring time delay in control input. The similarity in time delay between the two methods validates the application for use in laboratory experimentation.

#### **5.4.2 Pick-and-place control application validation**

The result of the pick-and-place application is an AR interface to run commands at specific locations for older models of robotic arms. The application is a simplified interface that any novice user can quickly adapt too and allows quick reprogramming for alternate positions. To run the application the user simply opens the HL2 application and chooses between picking at placing at one of two locations. The HL2 will automatically connect to the LEWIS control board upon opening the application, therefore all that is required of the user is the input. Figure 39 exhibits a flowchart of application operation.

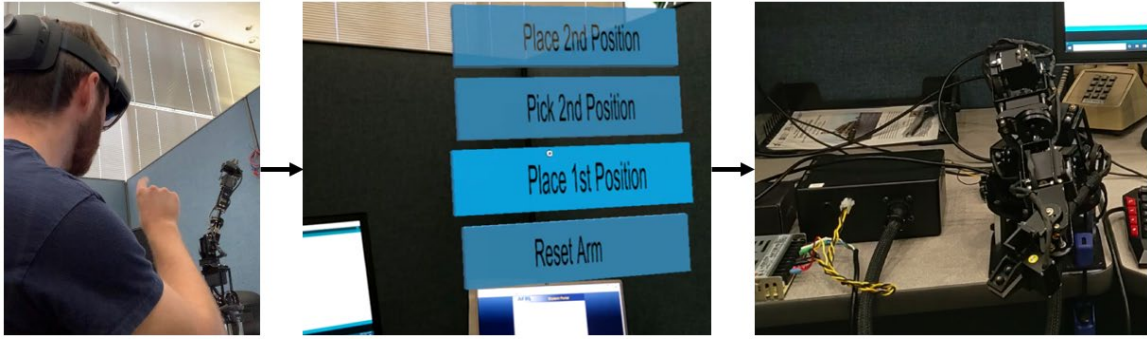


**Figure 39.** Flowchart of application operation.

The application was tested for repeatability by moving and placing a 3D printed object between the two defined positions for at least 15 repetitions. This setup is shown below in Figure 40. It was observed that in the same series of repetitions the robot did not fail to place the object, however across multiple, intermittent runs some error is induced. Thus the reset button is included in the interface, which resets the robot to its original position and therefore corrects the first and second positions.



**Figure 40.** Movement of 3D printed object first and second position.

The key contributions of this study can be summarized as follows:

1. Serves as a first-step investigation into an AR communication pipeline for servo commands and robotic control.

2. Successfully tested the repeatability of the specific robot arm with the AR commands, and this investigation led to the development of an additional commands to address issues with repeatability.

### 5.4.3 Gen3 move to target results

In order to test the viability of the position control application for the robot an experiment is designed to quantify the time it takes to deploy a sensor with the robot arm with and without AR. For the first session in the experiment, a novice user and an expert user attempt to move the arm to a specific vertical position. The novice user is defined as a subject with zero experience with control of the Gen3 and AR, and the expert user is defined as a subject with over six months of experience. The first session is designed as a first-step investigation into novice and expert control with and without AR and serves as an introduction for the novice. For the second session in the experiment, a target position on a metal structure is marked with a strip of tape, and a sensor box with magnetic attachment is held by the robotic arm and placed on the structure. A successful attempt is defined as attaching the sensor to the line, otherwise the result is not used. In both sessions the results of control with a physical controller are compared to AR. Figure 41 demonstrates this where the robot is approaching the target line on the metal surface with the magnetic sensor box.

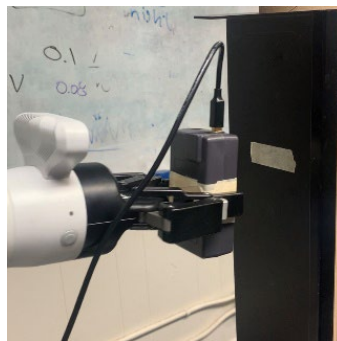


**Figure 41.** The robot with sensor approaching the target line.

The process starts with the robot at rest position for each test. The time between the start of control and target position success is measured and recorded for five tests. The user starts movement by manual control and time is recorded based on the user's cognition for the first session and the time of attachment for the second session. With AR the application is opened in the user's view and the user defines the robot origin and target position with the corresponding holograms. For the first session time is recorded manually and for the second session robot-held sensor data is recorded to measure time and demonstrate robot movement. For AR time includes the time to define the target position in the application, and this is added to the time it takes for the MATLAB code to move the arm to the defined target. The reported results include a time comparison between novice and expert for each session, and the average time for each control mode is calculated and reported. Figure 42 shows the time comparison for the novice versus expert for the first session.

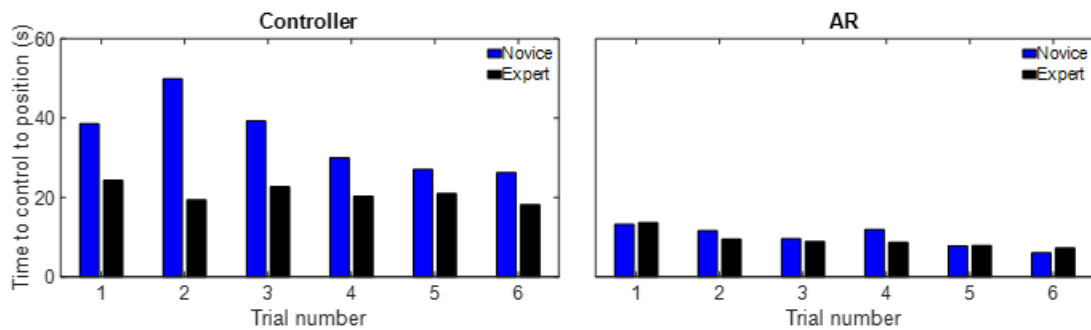


**Figure 42.** Control results for first session.

The results show a significant difference between the untrained subject and the trained subject when controlling the arm with the physical controller. On average with the controller the expert is nearly 10 seconds faster than the novice. However, with AR the two subjects are very similar in the time to deploy the sensor. Session two repeats this experiment, except now a target position on a metal structure is marked with a strip of tape

and a sensor box with magnetic attachment is held by the robotic arm and placed on the structure. Figure 43 displays the data collected from the robot-held sensor for the first manual control tests. Figure 44 shows the novice's improvement from first to second test, and the final three tests are reported in Figure 45. For Figures 43 and 44, the results for controller are plotted from first excitation to 0.5 seconds after the peak that indicates the sensor contacted the target surface. Figure 43 demonstrates a low-quality result where the novice and expert need to re-train themselves on the correct control path. Contact with the target surface is noticeably quieter with AR in the expert's attempt versus the novice. Figure 44 shows the next step in the experiment where both subjects improve in the time it takes to reach the target.

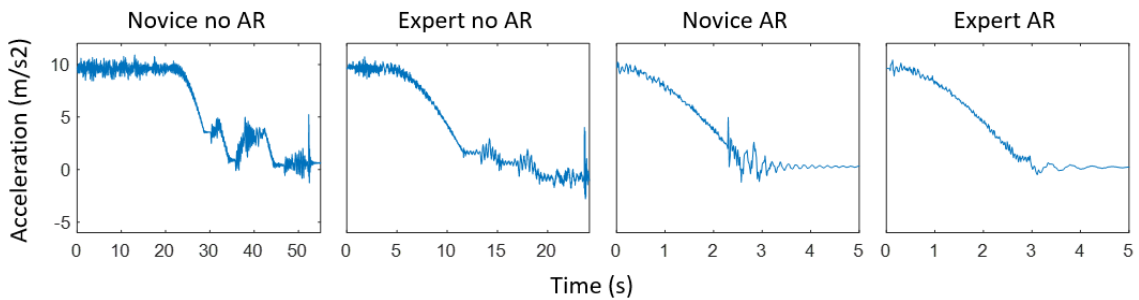


**Figure 43.** Time history of Test 1.

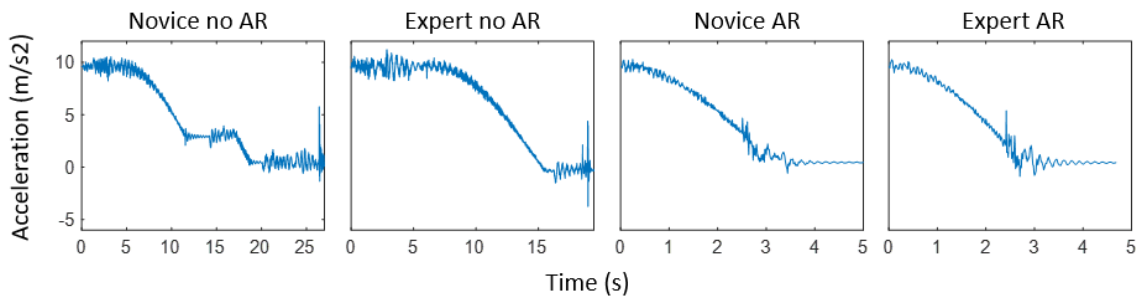


**Figure 44.** Time history of Test 2.

The results show improvement for both operators between Test 1 and 2, and also show a clear difference between novice and expert. The expert is nearly twice as fast in the

first test, having needed less time to re-train due to experience. The novice improves by nearly 25 seconds but is still slower than the expert. The final three tests are plotted in Figure 45. Here the time without AR is normalized to a 20 second period for each plot. The time to move with AR is unchanged for all four time histories, and the total time including target selection is reflected in Figure 46.

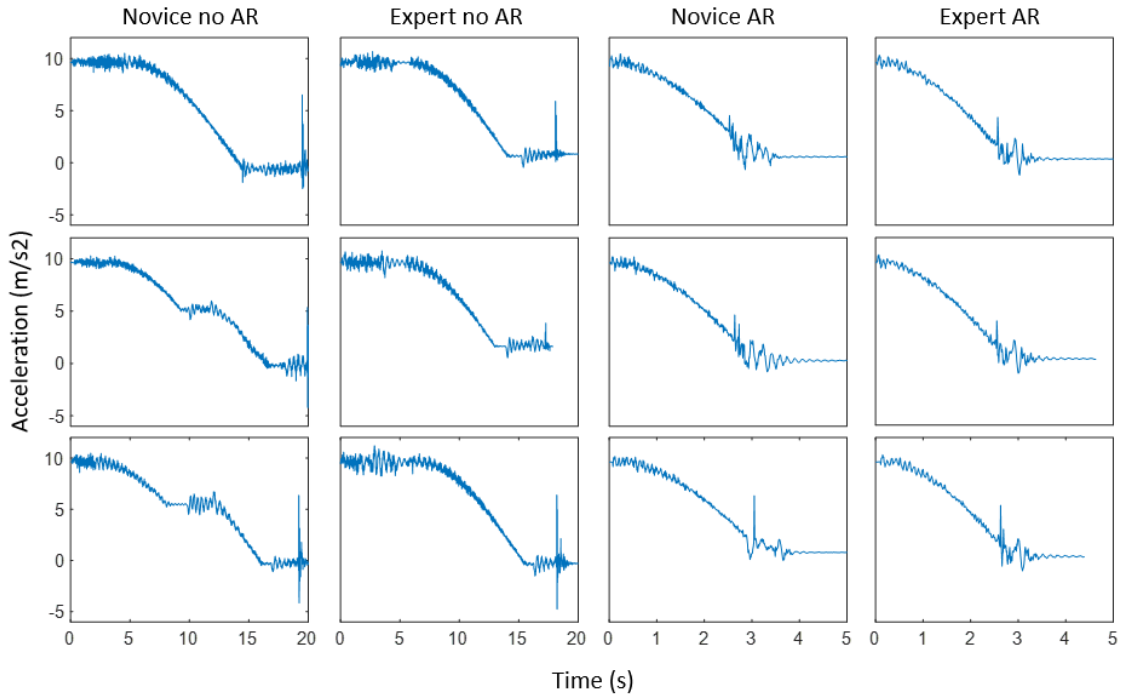


**Figure 45.** Time histories Test 3-5.

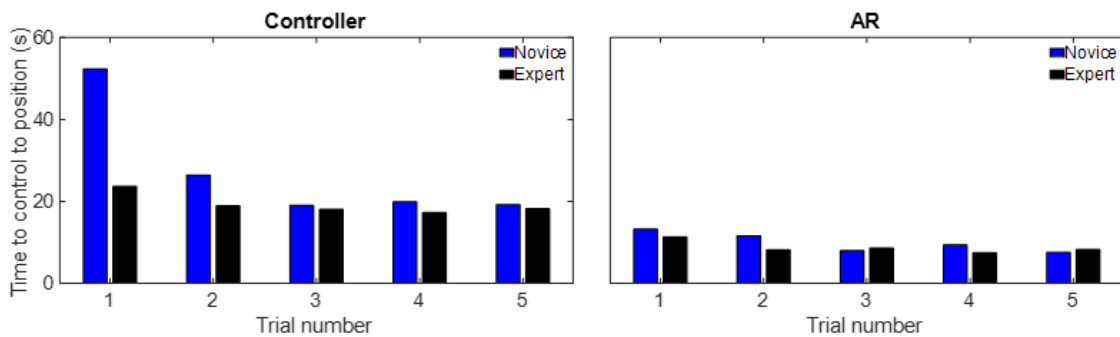


**Figure 46.** Control results for second session.

In this case, the novice improved much faster having already operated the robot in the first session. As was seen in the first session, the expert succeeded at a faster rate than the novice for the five tests, but the novice was much closer in time. Additionally, apart from the first trial, both novice and expert improved in time for the second session tests. Similar results were shown with AR as well, where again the novice performed efficiently from the start and was able to closely match the time of the expert.

#### **5.4.4 Gen3 frequency of movement results**

The experiment is designed to quantify the human's ability to follow platform movement represented by a shaker with and without the aid of AR. The goal of the human is to create a consistent, accurate frequency without breaching the robot's initial limit of 2 Hz. The second part of the experiment quantifies how accurately the robot matches the frequency of the platform movement. Preliminary results from Chapter 3 have reported that humans can best match frequency at under 3 Hz and improve when monitoring data in AR. This analysis also reported decreasing error when attempting to match higher frequencies. Therefore, the frequencies selected for this experiment range should range from 0-2 Hz, the maximum speed for the robot. Four values are selected at 0.5 Hz, 1 Hz, 1.5 Hz, and 1.9 Hz, where it is hypothesized that the human can match the frequency by moving themselves. A shaker is used as a reference frequency to represent a moving base. The user follows the movement of the shaker as closely as possible to replicate the response. This value is calculated by the sensor and the sensor acceleration plot and frequency calculation is shown in the user's view. As seen in Figure 47, the user maintains awareness of the reference frequency while following their own movement and monitoring output.

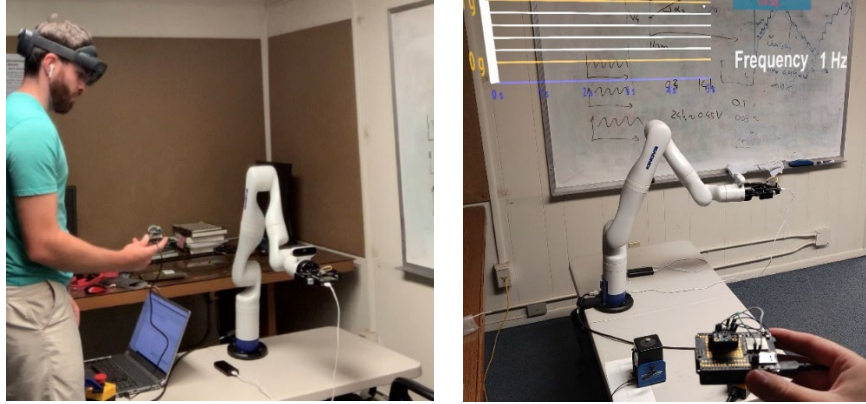


**Figure 47.** Experimental setup and user view of experiment.

The first part of the experiment runs for approximately one minute and the last 18 values are selected for the reported results, as for the first few values the user is adjusting to the setup. The test is repeated for each frequency for a total of four tests. Table 3 reports the recorded values at each frequency and states the number of threshold breaches.

**Table 3.** Frequency test results.

Shaker	0.5 Hz		1 Hz		1.5 Hz		1.9 Hz	
	No AR	AR	No AR	AR	No AR	AR	No AR	AR
1	0.53	0.55	1.05	0.97	1.64	1.52	1.91	1.92
2	0.42	0.58	1.04	1.03	1.51	1.55	1.73	1.96
3	0.69	0.41	0.77	1.05	1.55	1.54	1.89	1.99
4	0.32	0.64	0.81	1	1.55	1.6	1.93	1.88
5	0.43	0.55	1.02	1.02	1.71	1.49	2	1.94
6	0.61	0.24	1.04	1.07	1.81	1.5	2.09	1.91
7	0.5	0.55	0.91	0.88	1.53	1.55	1.95	1.99
8	0.47	0.38	0.97	0.97	1.5	1.49	1.9	1.94
9	0.3	0.38	1.12	0.99	1.5	1.57	1.98	1.94
10	0.21	0.45	1	1.06	1.5	1.52	1.89	1.96
11	0.65	0.53	1.02	1.05	1.51	1.55	1.97	1.85
12	0.44	0.52	1.1	1.03	1.53	1.55	2.08	1.98
13	0.3	0.51	1.03	1	1.59	1.49	1.71	1.91
14	0.47	0.54	1.05	1.02	1.51	1.53	1.9	1.95
15	0.49	0.53	0.94	1.07	1.44	1.43	1.93	1.89
16	0.34	0.54	0.94	0.88	1.58	1.51	1.96	1.95
17	0.46	0.48	0.92	0.97	1.54	1.53	2.01	1.85
18	0.42	0.52	1.1	0.99	1.56	1.54	2.06	1.93
Std. Dev	0.122	0.095	0.092	0.054	0.084	0.037	0.098	0.041

The error between human and reference is induced by a combination of human error and error in the FFT calculation. As shown in by the results, the user creates a frequency that is much more consistent with the aid of AR than without. Monitoring the frequency they are generating also helps the human ensure that the threshold is not crossed, meaning the robot is able to run without faltering. Without the knowledge imparted by visualization in AR, the user failed four times. Figure 48 reports the standard deviation for each dataset for the specified frequencies in the form of a bar graph.

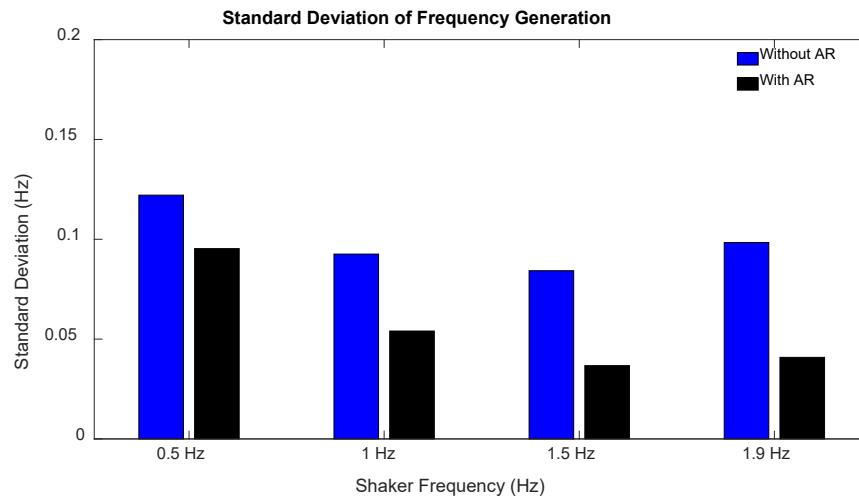


**Figure 48.** Results of frequency response experiment.

The human has the most difficulty at the lowest frequency of 0.5 but performs similarly at the three higher frequencies. With and without AR the human follows the same trend of improvement between 1, 1.5, and 1.9 Hz however there is a significant improvement at each individual value with AR. Row 13 is selected as the values to run for the robot, where the arm is setup holding the sensor box to record the acceleration values. These values are 0.51, 1, 1.49, and 1.91 Hz. Auto-spectral density estimates were generated for each output. This is done to determine the frequency of the robot movement to quantify

accuracy. The shaker frequency is also checked since it cannot be assumed to be exact, and this value is plotted as a vertical line in each PSD shown below in Figure 49.

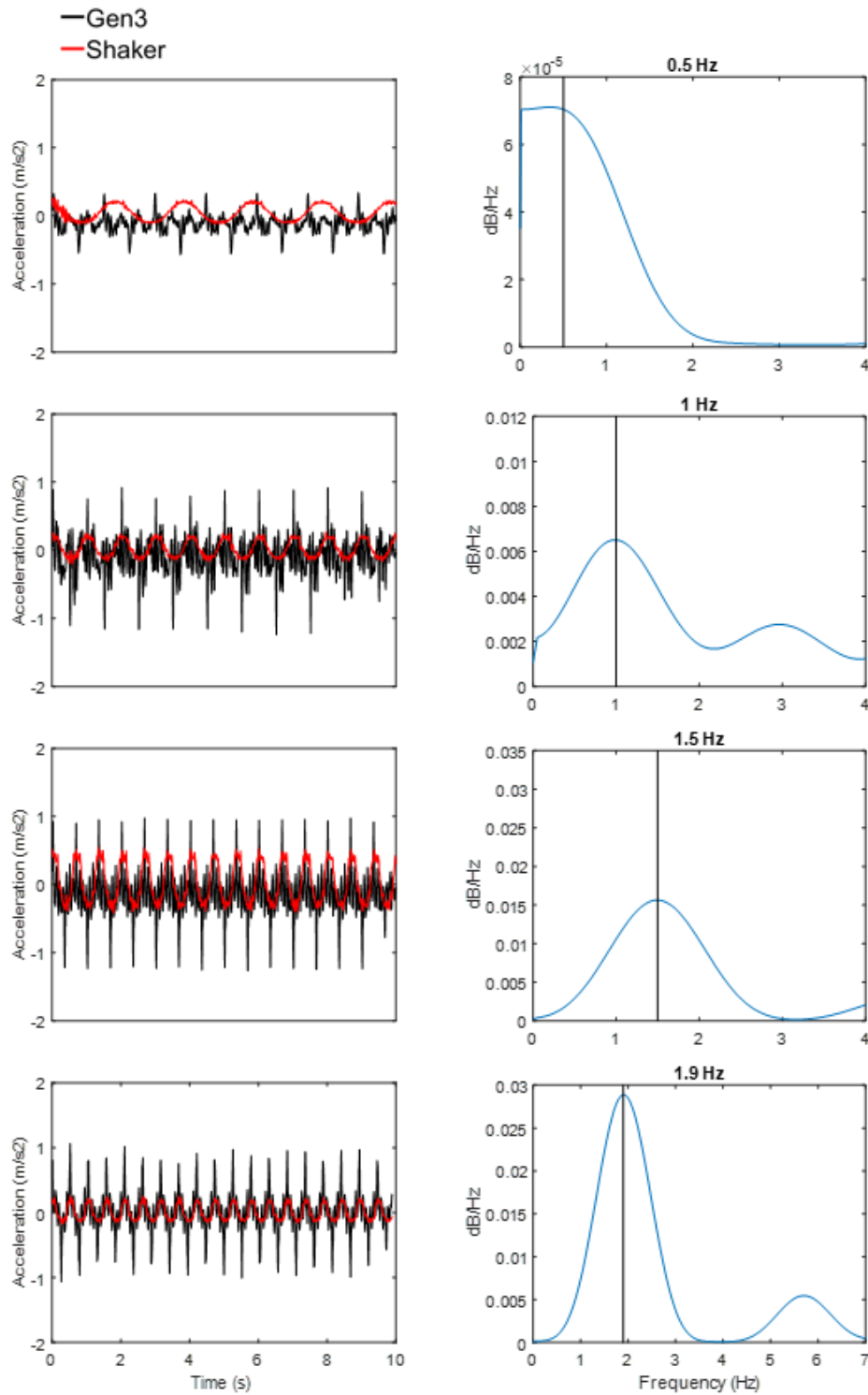


**Figure 49.** Results of robot movement at frequency.

The Gen3 arm performs very well at matching the shaker frequency for the three highest values. However, at 0.5 Hz it does not run as efficiently. As seen in Figure 49, the robot movement does not generate a smooth curve that is in synch with the shaker. Rather, the resultant PSD gives 0.4 Hz as the result for 20% error. This is due to the joint movement of the robot, which performs shaky motion at such low frequency. At higher frequency the robot moves with more stable motion while matching the frequency with less than 2% error. As a result, it can be concluded that the robot would be best implemented for frequencies between 0.5-1.9 Hz, and environments with higher level of vibration should be avoided. Future work would see an implementation of the same framework where instead of running at an arbitrary time the robot is set to offset the movement exactly. The contributions of the Gen3 control applications are as follows:

1. Two AR applications are developed to apply robotics to sensor deployment tasks.
2. The applications emphasize user awareness of the physical space by augmenting control and sensor feedback.
3. The reported experiments prove that complex control is simplified with AR as the novice can compete with the expert in the total time to deploy a sensor.
4. Frequency control is tested with AR where the user can better create a consistent frequency without breaching a limit, where the Gen3 can then match this frequency closely.

## **Chapter 6. AR Tools for Robotic Ground Vehicle Tasks**

### **6.1 Methodology of AR Application for Robotic Vehicle Tap Testing**

Rockfalls are a frequent geological hazard worldwide that must be investigated and studied for prevention measures (Ma et al., 2021). The rock blocks originating from a rockfall range from small gravel to large boulders, and as Figure 50 demonstrates how this poses a significant threat to infrastructure and human activity (Singh et al., 2016). Inspectors conduct tasks to predict threats, and in doing so are at risk themselves. The inspector wants to maintain a safe distance from the rockface to avoid potential rockfall. Another factor to consider that influences the safety of inspectors is visibility. Environments with restricted visibility can be dangerous for humans as it can eliminate any knowledge of the current situation, putting the human at risk of tripping over obstacles or losing their orientation (Fritsche et al., 2017). In other situations with restricted visibility the human may not be able to access or see an area of interest, therefore mobile robots can provide access (Flann et al., 2002). This research seeks to provide a mode of accurate control for a mobile robot in any inspection scenario, including those in which the inspector may not have full awareness. In a similar sense, gaze distraction can be an issue. Humans receive approximately most of the information they process through vision, and this information is best perceived in central vision. Each mental task reduces the capacity for other simultaneous tasks and humans, therefore it is important that an inspector's focus remains on the ground vehicle in our case. The previously listed challenges can be overcome by deploying a mobile ground vehicle for inspection with the aid of AR technology.

For ground vehicles such as Brutus, obstacles such as rocks and ledges pose the greatest risk to the robot. Obstacle avoidance must be preprogrammed into the control system to avoid damage to the robot (Chacko et al., 2020) but in a new environment it is not possible to program environment obstacles into the robot control on the fly. AR markers are suitable for manually defining object detection and path planning, but the system as a 2D or 3D approach is not scalable as the number of objects increases. Rather than automation, manually controlling the robot in the AR interface is advantageous as human cognition can easily adapt to obstacles in the environment. For example, AR has been applied to robot teleoperation to reduce gaze distraction where augmenting live video feed from the robot limits the user's view to pertinent information for safer, more controlled operation (Hedayati et al., 2018). By combining AR technology with human cognition obstacle avoidance is addressed as a barrier to robotic operations.



**Figure 50.** Rockfall danger to infrastructure and civilians.

### **6.1.1 Hardware components of Brutus application**

Brutus, a remoted-controlled ground vehicle, was developed to enable automatic classification of rock crack characteristics in the field (Nasimi et al., 2022). Distributed surfaces have been tested with the machine to eliminate inspectors' subjective judgements,

and to automatically classify the test surface. The following section describes the hardware components constructed to accomplish such tasks.

### **Main body components**

The entirety of the Brutus build is controlled by Arduino UNO which is connected to the gear box motor through a HiLetgo Motor Driver Controller board. The build also includes control of the tapping device, built with a four-bar linkage crank rocker. The purpose of this mechanism is to mimic the manual tapping motion of a human inspector that occurs when a test is being conducted in the field. Brutus includes a Raspberry Pi computer which enables a wireless connection to be made with the robot to enable modes of control outside of the standard handheld controller. These components can be seen in Figure 51. For new users, the handheld controller is not intuitive. Some form of training must be conducted first to ensure the operator is fully capable of understanding the large remote controller, which includes more than a dozen switches, joysticks, and buttons. For basic control, the most important modes are steering, propulsion, and braking. The AR interface consolidates control into these three categories to avoid overwhelming the user's cognitive load, especially if not an expert. The interface includes control to drive the robot forward, control to slow the robot to a stop and at maximum reverse, and steer the robot left and right.

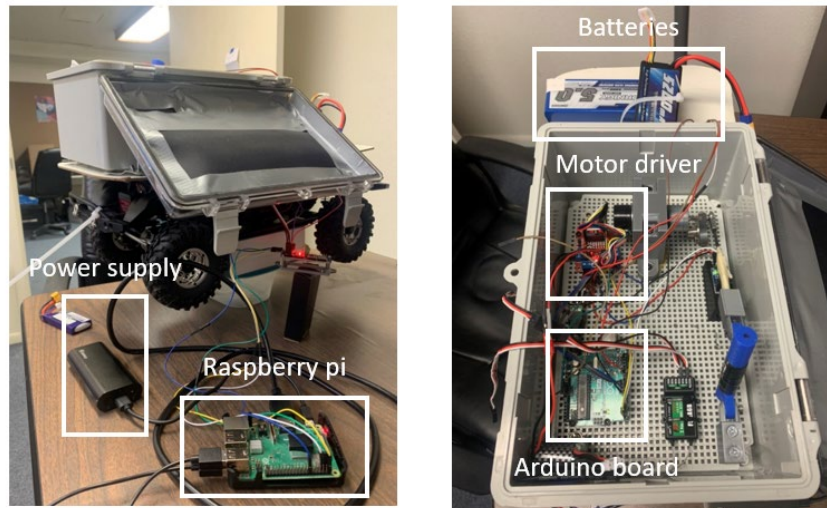


**Figure 51.** Brutus construction.

## Tapping mechanism

The crank rocker mechanism generates an acoustic response by moving the hammer in a specific motion. This mechanism consists of a gear box motor, crank wheel, rocker, rocker arm, coupler, and two position sensors. The tapping mechanism is driven by a 12 V gear box motor coupled with a larger crank wheel. The crank and motor mechanism is connected to the rocker arm by a coupler bar that translates the motion of the motor and crank wheel to the rocker arm. As the motor turns, the rocker arm moves forwards and backwards through the specified range of motion. As the rocker arm moves, position sensors are used to track the total number of times the rocker mechanism has completed a cycle and track the home position. Once the preprogrammed number of cycles is completed, the rocker arm returns to the home position. The Arduino code specifies how many times the rocker arm must cycle before returning to the home position. A plastic housing component is mounted atop the Redcat chassis containing most Brutus components. The Brutus tap testing device consists of a TSINY motor, a rocker arm mechanism (Four-Bar Rocker and

Steel Ball Knob), a motor controller, two position sensors, Raspberry Pi 3 computer, an Arduino UNO, and Li-Po batteries. The tapping mechanism can be viewed in Figure 52 and the component breakdown is given in Table 4.

**Table 4.** Brutus component breakdown.

Part	Description	Manufacturer	Price
Arduino UNO	Microcontroller	Adafruit	\$23.00
HiLetgo Motor Driver	Controls servomotors	HiLetgo	\$9.49
Raspberry Pi 3	Computer	Adafruit	\$35.00
Headers	Connectors	Sparkfun	\$1.50
Jump wires	Connectors	Sparkfun	\$1.95
Redcat RC Crawler	Vehicle frame	Redcat	\$329.99
Lipo Batteries	Battery supply	Zeee	\$38.99
<b>Total Cost</b>			<b>\$439.92</b>

### **Sonar sensor**

As shown in Figure 52 the Brutus assembly includes a sonar sensor. The sonar sensor is built as part of the LEWIS series, titled LEWIS Sonar. LEWIS are versions of standard wireless smart sensors that allow for high versatility while minimizing cost and maximizing energy efficiency. LEWIS Sonar measures the distance to the target object by emitting ultrasonic sound waves which are reflected back and converted to an electric signal. For this project the sensor was built to track and gauge the distance between Brutus and the rockface. There are nine components in LEWIS Sonar, which are explained in the sections below. The sonar sensor components can be seen in Figure 53.

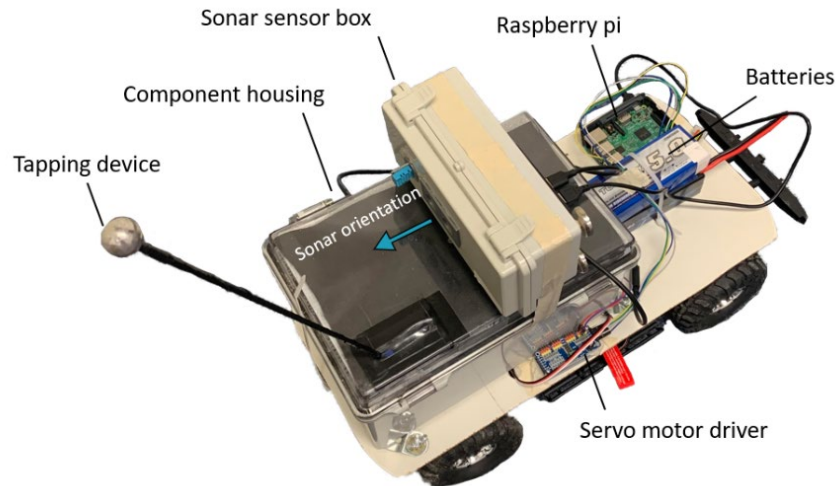


**Figure 52.** Full Brutus assembly including the sonar sensor.

The first component of LEWIS Sonar is the Arduino UNO, a microcontroller board with 14 digital input/output pins, a 16 MHz ceramic resonator, a USB-B connector, a power connection, and a reset button. All the data captured from the sonar sensor is computed by the Arduino UNO, which executes the code written in the Arduino IDE. The Adafruit AirLift WiFi Shield, the second part of the sonar sensor, is paired with the UNO. The Airlift WiFi Shield allows the use of the ESP32 chip as a WiFi co-processor. The UNO does not have WiFi built in, so the addition of the shield permits WiFi network connection and data transfer to the database and website where the sonar data is stored. The shield includes a microSD card socket used to host or store data. The shield is connected to the UNO with stack headers. The third component is the solar charging circuit, which is an Adafruit Solar Lithium Ion/Polymer Charger. The solar charging circuit is gathers power from a solar panel and transmits it to the fourth component, the battery. For the designed experiment no solar panel is used and instead the battery is pre-charged. Energy is subsequently transmitted from the battery to the load. The necessary voltage must be raised because the solar charging circuit's output voltage remains under 5V. Therefore, a Buck Boost

Converter is included in the assembly as the fifth component, which will boost voltage to 5V so the Arduino can operate.

A USB-A Breakout Board, which effectively serves as an adaptor to power the UNO, is the sixth component of the sonar sensor. The breakout board and UNO must be connected via a USB-A to USB-B connector. Jumper cables are required to connect the sonar sensor (Ultrasonic Distance Sensor HC-SR04), once the Arduino and WiFi shield are operational. The sonar sensor, the system's seventh component, is paired with the eighth component. This is a 3D-printed case that secures the sonar sensor inside the lid of the housing component, with the sensor oriented outward from the box. The ninth and final component of the sonar sensor is a base frame that was also 3D printed to address cable management concerns and secure the other individual components.

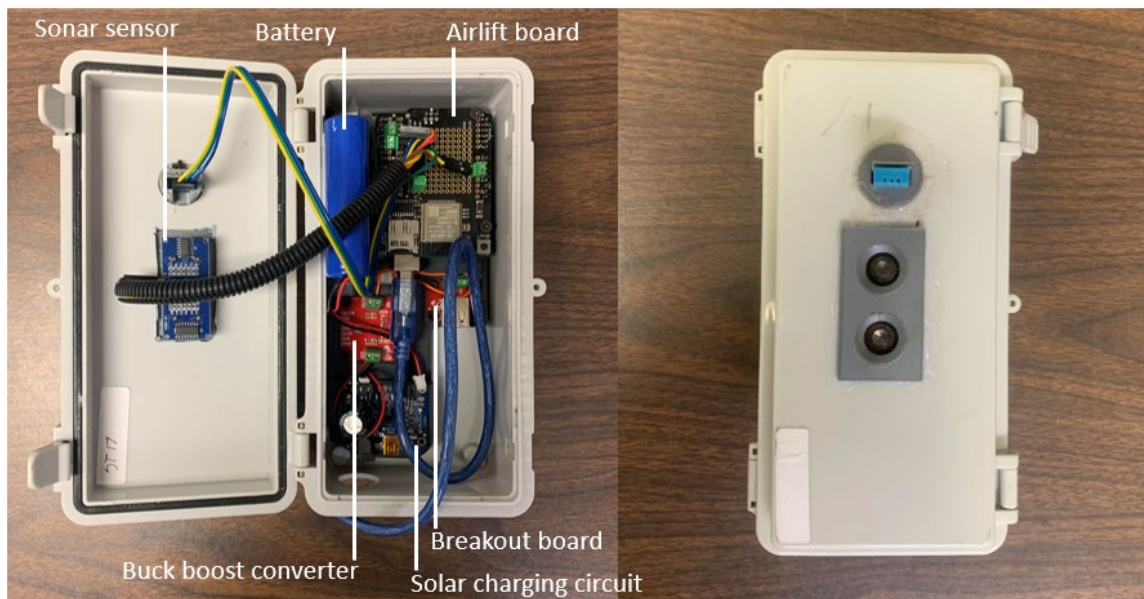


**Figure 53.** Sonar sensor components.

### **6.1.2 Software components of Brutus application**

Brutus software development makes it possible to interface between the control mode of the robot and an AR command hub, which is established in a head-mounted device. The following sections explain the development of software implemented in the Brutus platform. Figure 54 demonstrates the goal for application development and implementation, where a user controls Brutus based on sonar sensor feedback. Hand tracking and manual movement of a digital twin for moving a robotic arm has been demonstrated with AR technology (Manring et al., 2020), but the inaccuracy associated with this mode of control is not suitable for operations such as precise movement of robotic arms. However, this method is viable for ground vehicle control as it depends on human cognition for safe control of speed and direction that directly correlates to the human's movement. Manipulation of a robotic ground vehicle with this method depends less on precision for safety making it a useful mode of control. Because the holograms for speed and direction control of Brutus follow the movement of the human's hand, it is significantly easier to control speed and positioning instinctively because the human is operating based on their own perception and feeling. The holographic interface for control of the ground vehicle includes three holograms with specific functions and one button that activates the tapping mechanism. The first hologram controls the propulsion of the vehicle, thus at its maximum distance the vehicle moves forward at the highest allowable velocity. Manipulation of the hologram forwards and backwards controls the amplitude of the velocity, therefore slower hand movement by the user correlates to reduced acceleration and velocity of the robot. The same goes for braking, where the user slows the movement of the robot by their hand movement and can activate a complete stop by moving the

hologram to its maximum value. Furthermore, the robot is guided by the third hologram which controls turning laterally in each direction. Again, as the human manipulates the hologram in either direction the robot reacts accordingly in the exact same manner, allowing the user to make extreme turns or slight adjustments according to their own intuition. On the right side of the interface the reading from a sonar sensor equipped to the robot is displayed. This provides the human with all the information they need to control the robot to the correct distance from the test surface.

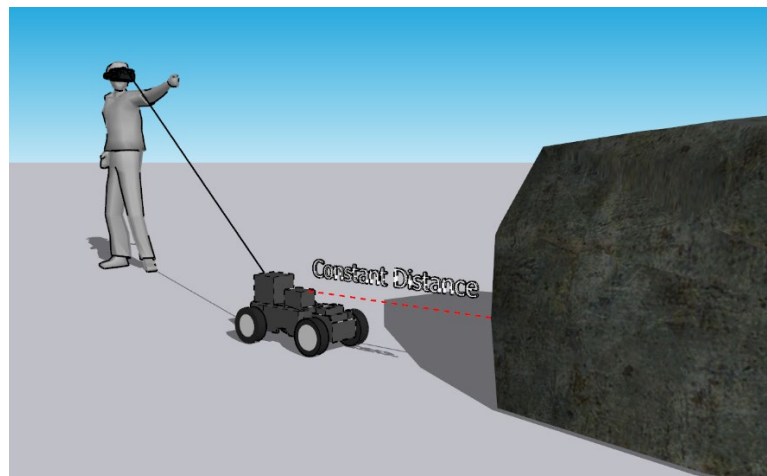


**Figure 54.** Initial goal for application development.

Development of the Brutus control application is done in Unity version 2019.4.20f1. Cylindrical 3D objects are placed into the scene to be used as the holograms for control of the robot. These objects are configured for HL2 deployment by ManipulationHandler scripts from MRTK version 19.0.02 from Microsoft. These scripts make it possible for the human to interact with the holograms that spawn in their field of view and within their grasp. Hand tracking is done by the HL2 depth sensors which allows the human to perform simple motions to securely grab each hologram with low error, where the tracking allows the human to move the hologram according to their own hand movement. The control holograms are populated as Rigid Bodies where constraints can be

applied to each hologram based on their axis of movement to constrict rotation, translation outside of the path, and bounds. The Drive component translates in the y-plane and the Steer component translates in the x-plane. Movement of each hologram updates a value based on the length of movement. This value is communicated to the Raspberry Pi, programmed in Python, which is setup as a server on a WiFi hotspot for field use. The values sent from HL2 are received and the Brutus servomotors controlling steering, driving, and tapping respond. Programming of the servomotor control was done in the Python program on the Raspberry Pi. Eye tracking is included in the application as a means of assessing the application in the field. When start is selected in the eye tracking menu, the HL2 sensors begin storing eye gaze data in a MySQL database for future analysis. These components can be seen in Figure 55 and the view in HL2 can be seen in Figure 56.

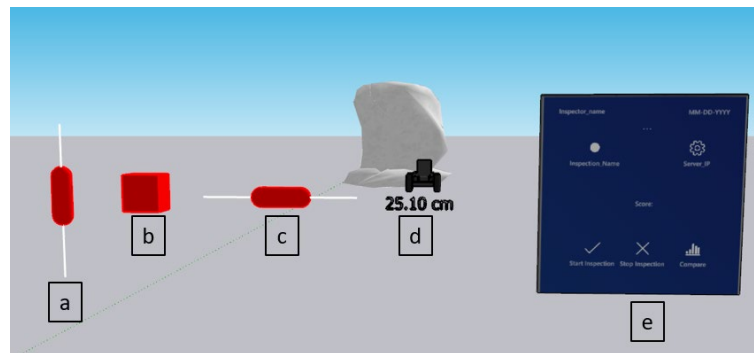


**Figure 55.** Application components; (a) Drive hologram; (b) Tap hologram; (c) Steer hologram; (d) Sonar reading; (e) Eye tracking menu.

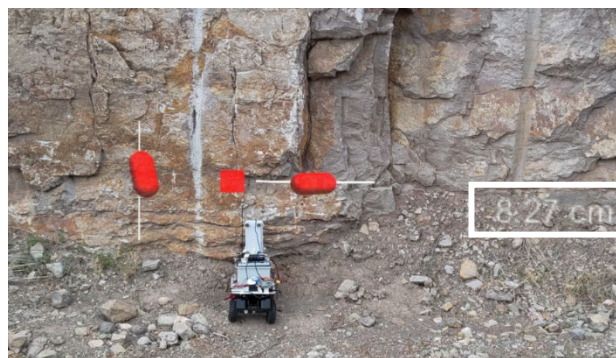


**Figure 56.** Example of view in HL2 with working sonar display.

## 6.2 Tap Testing Control Application Implementation

The result of AR application development for tap testing of structures is an interface that includes control of a mobile ground robot and sensor data to fully inform the user. To implement the application in the field a test was conducted at a rockface in Tijeras, New Mexico with a mobile WiFi hotspot for sensor-AR and robot-AR communication. This site was of interest due to its high potential for rockfall hazards along the roadcut. The proposed system does not measure input vibration as in traditional approaches; instead, the system analyzes sound waves reflected from the rock surface. Two locations were selected along the roadcut wall designated Position 1 and 2. These locations were very close to each other, where Position 1 was visually identified as having a crack and the Position 2 was free of damage. Figure 57(a) shows the location of the experiment and includes the first location marked with green marker in Figure 57(b). Figure 57(c) shows the view of the HL2 control panel with Brutus.



**Figure 57.** (a) Rockface location; (b) Position 1 location; (c) Brutus control view in HL2.

### 6.2.1 Tap testing experiment results

Five parameters were recorded as part of the validation experiment. These parameters are chosen to reflect the safety of the inspector and the success rate of the AR application versus control without AR. These parameters are:

1. Distance to wall – consistency AR vs no AR.
2. Distance person to Brutus.
3. Time to reach position.
4. Gaze distraction quantified by eye tracking.

Each parameter was recorded during the course of two tests at each location. On the day of the experiment the sonar sensor website went down, thus the only viable results from the test are parameters 2-4 as 1 is based on the feedback from the sonar sensor. Conclusions can still be drawn from parameters 2-4 in terms of understanding the safety of the inspector and the ease of control in AR versus the traditional method of remote control. As shown in Figure 56 the researchers returned to the site at a later date to briefly confirm the success of the sonar sensor component of the Brutus control application. The first report result is eye tracking in Figure 58. For approximately 1000 data points at a sampling rate of approximately 34, a comparison is drawn between the different modes of control.

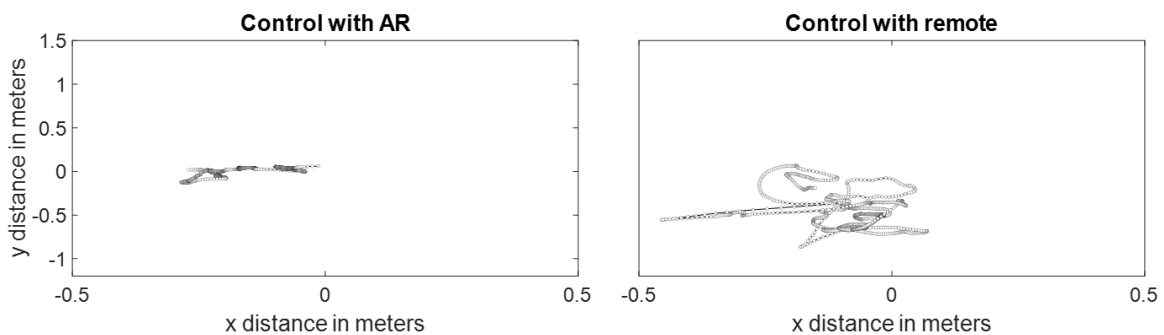


**Figure 58.** Eye gaze results for Brutus test.

The eye gaze results show a significant difference between AR and remote control. As hypothesized, AR reduces the human’s focus to a small area which encompasses the control panel for Brutus. With the control panel augmented directly on top of the robot the user need not look away. When holding the remote for Brutus control, the human’s eyes cover a considerably larger region with a more random pattern. The time to control the robot to the target position and the distance of the user to the robot is reported in Table 5, where distance is measured with a tape measurer and time is report from recorded video.

**Table 5.** Experimental results for operator safety and ease of control.

	With AR		Without AR	
	Test 1	Test 2	Test 1	Test 2
Distance: user to Brutus	472 cm	516 cm	268 cm	290 cm
Time to reach target	18.3 s	16.1 s	17.7 s	17.3 s

The results of the reported experiment are meant to quantify the safety of the inspector and the ease of control in AR versus the traditional method of remote control. As reported, the time to drive Brutus to the desired target is similar with AR versus with the remote control. However, the user felt it necessary to follow along with the robot when controlling with the remote control. With AR the user was barely displaced from their starting position. This result can be improved even further by the working sonar distance, as this will alleviate the user’s need to monitor the robot position relative to the test surface. Additionally, the repeatability is expected to improve by receiving and ensuring the same position is retained for each deployment. Future work for this application will include a field deployment with proper functionality of the sonar network to investigate all five parameters. The summary of the key contributions of this section are as follows:

1. Physical prototype of an acoustic SHM method deployed on a mobile ground robot that is constructed with sensors to improve the original method.

2. Direct augmentation of sensor data measuring a distance, which is applied to an acoustic SHM method.
3. A new control method for a mobile ground robot that directly augments steering, driving, and tap test actuation controls to reduce gaze distraction compared to a traditional remote controller.
4. The viability of the application for field deployment was quantified by an experiment at a rockface in New Mexico where the subject successfully controlled the Brutus robot to tap test the rock surface with AR.

## **Chapter 7. Conclusions**

This thesis has provided the framework for applying Augmented Reality tools to engineering tasks including inspection, experimentation, data feedback, and control. The domain of this research is in SHM and infrastructure engineering. A head-mounted device was used for this research to deploy and operate the developed AR applications.

### **7.1 AR for Engineering Tasks Conclusions**

This thesis considers the importance of human-centered framework where often experts in SHM prefer to be present to make decisions based on their own cognition rather than rely solely on artificial intelligence or other independent algorithms. The research solves a problem with HCI where the operator experiences gaze distraction when attempting to monitor data and dynamic events. AR provides additional information to the AR user via HMD, which allows the user to continue to operate and observe the physical space without impedance. This thesis focuses on visualization and control as two primary areas of AR development. First the author presents a preliminary study in which an application is developed for sensor-AR communication. The result shown enables the research community to design, program, and examine new AR applications interfacing sensor feedback with real structures and environments. This study motivated the rest of the body of work which includes five AR applications based on the same research approach.

The result of the first application is an interface for sensor feedback and control of actuators in vibratory experimentation. The application is developed to plot sensor data in an interface complete with voltage, frequency, and duration controls for vibration

generation. The results of the experiment prove that AR control responds at a similar rate to that of a direct wired connection, making it a viable solution for experimentation.

The area of robotics is of interest for use in dynamics as well. This area of interest for human-centered tasks related to SHM. The result of this research was two applications developed for feedback and control of robotic arms in AR for the purpose of sensor deployment. The results of the reported experiments verify the repeatability and accuracy of the proposed methods. Additionally, it was shown that AR improves a human's sense of movement when generating frequency themselves, and this frequency was measured by a handheld sensor. By communicating this value to the Gen3 arm, the results show that it is possible to use a human-centered approach to stabilize a robotic arm attached to a dynamic base. The frequency control and position control applications serve as important first-step research into AR and robotic arm control. In future work, the author would look to incorporate higher-level feedback into the application. For example path planning visualization, collision avoidance, joint control, and matching the base movement of a real moving structure are of interest.

This MS thesis also presented an AR application for an SHM method using a mobile robot titled Brutus. The Brutus robot is constructed with a sonar sensor to measure the distance between the robot and test surface. Augmenting the control interface with the sonar sensor reading fully informs the user for high-level control of the robot deployment. The results of the reported experiments indicate that the augmented interface narrows the inspector's focus for more efficient and informed task conduction while also increasing the safety of the inspector. Using the framework developed in the thesis, AR applications can now be developed for other domains interested in direct feedback to improve human

cognition including, but not limited to; aerospace engineering, satellites, robotics, healthcare, human-centered smart buildings, machine health monitoring, and vehicles.

## **7.2 Recommendations**

While this thesis seeks to address SHM needs with novel tools including AR and low-cost sensors, there are inherent shortcomings that should be considered. The adoption of AR technology for field implementation and everyday use is not certain due to the current state of the hardware. Based on the work conducted in this thesis and interaction with industry professionals at national labs including LANL and AFRL, the following factors are recommended to accelerate the implementation of AR technology in SHM:

1. Improvement in hardware.
  - a. Common failures associated with the hardware include poor visibility in bright conditions and overheating. This causes problems that make it difficult to implement the technology for use in the field. A decrease in size and weight would also make the hardware more viable for everyday use. Addressing these issues would make the technology more feasible for SHM.
2. Increase processing capacity.
  - a. The low processing capacity of the headset is not unexpected since the housing component has limited room and improvement would be costly. However, many applications have trouble running and suffer from poor framerates along with other processing issues that could see improvement in the future.
3. Cost reduction for owner.

- a. A major roadblock to widespread use is the cost of the devices. Current HMD AR devices cost thousands of dollars which is not viable for the average household and can be too expensive to be considered for research groups.

### **7.3 Publications**

The results of this research are either published or in the process of publication in journals, conference proceedings, and other medium.

#### **a. Journal Publications**

**Wyckoff, E., Ball, M., & Moreu, F. (2022).** Reducing gaze distraction for real-time vibration monitoring using augmented reality. *Structural Control and Health Monitoring*. <https://doi.org/10.1002/stc.3013>.

Published May 24, 2022.

**Wyckoff, E., Ball, M., & Moreu, F. (2022).** Feedback and Control in Dynamics and Robotics using Augmented Reality Applications.

Planned submission: *Advanced Engineering Informatics*, August 2022.

**Wyckoff, E., Ball, M., Hanson, J.W., Reza, R., Olaguir, E., & Moreu, F. (2022).** Augmented Reality Tools for Robotic Ground Vehicles and Structural Tap Testing

Planned submission: *Automation in Construction*, August 2022.

#### **b. Conference Proceedings**

**Wyckoff, E., Ball, M., & Moreu, F. (2022).** Real-Time Human Cognition of Nearby Vibrations Using Augmented Reality. In: Grimmelsman, K. (eds) *Dynamics of Civil Structures, Volume 2. Conference Proceedings of the Society for Experimental Mechanics Series*. Springer, Cham. [https://doi.org/10.1007/978-3-030-77143-0\\_14](https://doi.org/10.1007/978-3-030-77143-0_14).

**Wyckoff, E., Khorasani, A., Malek, K., & Moreu, F. (2022).** Increasing the use of Human-Machine Interfaces with Augmented Reality for Inspectors. *Conference Proceedings of the International Conference on Bridge Maintenance, Safety and Management*.

### **c. Book Chapters**

Mascareñas, D., Moreu, F., **Wyckoff, E.**, Susmita, S., & Morales, J. (2022). Augmented reality for cradle-to-grave infrastructure monitoring, and inspection. *Recent Developments in Structural Health Monitoring and Assessment — Opportunities and Challenges*, 407–428. [https://doi.org/10.1142/9789811243011\\_0014](https://doi.org/10.1142/9789811243011_0014).

### **d. Technical Reports**

Khorasani, A., Susmita, S., Cowan, A., Malek, K., Sanei, M., **Wyckoff, E.**, Moreu, F., & Law, V. (2022). Human-Machine Interfaces of New Technologies and the Railroad. (Federal Railroad Administration). Technical Report.

Malek, K., **Wyckoff, E.**, Khorasani, A., Susmita, S., Moreu, F., & Law, V. (2022) Stage I Report. Augmenting Reality for Safer Inspections of Railroad Infrastructure and Operations. (Transportation Research Board). Technical Report.

### **e. Magazine Articles**

Moreu, F., Malek, K., **Wyckoff, E.**, & Khorasani, A. (2022). Augmented Reality Existing Capabilities and Future Opportunities. *TR News*.

## References

- Andersson, N., Argyrou, A., Nägele, F., Ubis, F., Campos, U. E., De Zarate, M. O., & Wilterdink, R. (2016). AR-enhanced human-robot-interaction-methodologies, algorithms, tools. *Procedia CIRP*, 44, 193-198.
- Aguero, M., Maharjan, D., Rodriguez, M. D., Mascareñas, D. D., & Moreu, F. (2020). Design and Implementation of a Connection between Augmented Reality and Sensors. *Robotics*, 9(1), 3. doi:10.3390/robotics9010003.
- Azeem, N., Yuan, X., Raza, H., & Urooj, I. (2019). Experimental condition monitoring for the detection of misaligned and cracked shafts by order analysis. *Advances in Mechanical Engineering*, 11(5), 1687814019851307.
- Ballor, J. P., McClain, O. L., Mellor, M. A., Cattaneo, A., Harden, T. A., Shelton, P., & Mascareñas, D. D. (2019). Augmented reality for next generation infrastructure inspections. In *Model Validation and Uncertainty Quantification, Volume 3* (pp. 185-192). Springer, Cham.
- Bateman, S., Mandryk, R. L., Gutwin, C., Genest, A., McDine, D., & Brooks, C. (2010). Useful Junk? The Effects of Visual Embellishment on Comprehension and Memorability of Charts. *Proceedings of the 28th International Conference on Human Factors in Computing Systems - CHI '10*. <https://doi.org/10.1145/1753326.1753716>.
- Behzadan, A. H., Dong, S., & Kamat, V. R. (2015). Augmented reality visualization: A review of civil infrastructure system applications. *Advanced Engineering Informatics*, 29(2), 252-267.
- Čala, M. (2015) "Control system for a small electrodynamic exciter," Proceedings of the 2015 16th International Carpathian Control Conference (ICCC), pp. 64-68, doi: 10.1109/CarpathianCC.2015.7145047.
- Carment, L., Abdellatif, A., Lafuente-Lafuente, C., Pariel, S., Maier, M. A., Belmin, J., & Lindberg, P. G. (2018). Manual dexterity and aging: A pilot study disentangling sensorimotor from cognitive decline. *Frontiers in Neurology*, 9. <https://doi.org/10.3389/fneur.2018.00910>.
- Ceriotti, M., Mottola, L., Picco, G. P., Murphy, A. L., Guna, S., Corra, M., et al. (2009). Monitoring heritage buildings with wireless sensor networks: The Torre Aquila deployment. In *Proceedings of ACM/IEEE IPSN* (pp. 277–288).
- Chacko, S. M., Granado, A., RajKumar, A., & Kapila, V. (2020, October). An Augmented Reality Spatial Referencing System for Mobile Robots. In *2020 IEEE/RSJ International Conference on Intelligent Robots and Systems (IROS)* (pp. 4446-4452). IEEE.
- Chi, H.-L., Kang, S.-C., & Wang, X. (2013). Research trends and opportunities of augmented reality applications in architecture, engineering, and construction. *Automation in Construction*, 33, 116–122. <https://doi.org/10.1016/j.autcon.2012.12.017>.
- Chow, J. C., Detchev, I., Ang, K., Morin, K., Mahadevan, K., & Louie, N. (2018). Robot vision: calibration of wide-angle lens cameras using collinearity condition and k-nearest neighbour regression. *arXiv preprint arXiv:1810.00128*.
- Deka, L.; Chowdhury, M.A. (Eds.) *Transportation Cyber-Physical Systems*; Elsevier: Amsterdam, The Netherlands, 2019.

- Dick, E. (2021). The Promise of Immersive Learning: Augmented and Virtual Reality's Potential in Education. *Information Technology and Innovation Foundation. Discover Our Gen3 Robots*. Kinova. (n.d.). Retrieved June 22, 2022, from <https://www.kinovarobotics.com/product/Gen3-robots>
- Fang, H. C., Ong, S. K., & Nee, A. Y. (2014). Novel AR-based interface for human-robot interaction and visualization. *Advances in Manufacturing*, 2(4), 275-288.
- Flann, N. S., Moore, K. L., & Ma, L. (2002). A small mobile robot for security and inspection operations. *Control Engineering Practice*, 10(11), 1265-1270.
- Flick, J. (2020, September 23). Building a Graph. Retrieved from <https://catlikecoding.com/unity/tutorials/basics/building-a-graph/>.
- Fritsche, P., Zeise, B., Hemme, P., & Wagner, B. (2017, October). Fusion of radar, LiDAR and thermal information for hazard detection in low visibility environments. In *2017 IEEE International Symposium on Safety, Security and Rescue Robotics (SSRR)* (pp. 96-101). IEEE.
- Hedayati, H., Walker, M., & Szafir, D. (2018). Improving collocated robot teleoperation with augmented reality. *Proceedings of the 2018 ACM/IEEE International Conference on Human-Robot Interaction*. doi:10.1145/3171221.3171251.
- Harvey, P. S., & Elisha, G. (2018). Vision-based vibration monitoring using existing cameras installed within a building. *Structural Control and Health Monitoring*, 25(11). <https://doi.org/10.1002/stc.2235>.
- HoloLens 2-Overview, Features, and Specs: Microsoft HoloLens*. (2022). Overview, Features, and Specs | Microsoft HoloLens. (n.d.). <https://www.microsoft.com/en-us/hololens/hardware>.
- Horbst, J. (2020). GoHolo. [Thesis]. University of Applied Sciences Technikum Wien.
- Hui-Ping, L., Dai-min, C., & Miao, Y. (2011, August). Communication of Multi-robot System on the TCP/IP. In *2011 International conference on mechatronic science, electric engineering and computer (MEC)* (pp. 1432-1435). IEEE.
- Hunter, N. F., Cross, K. R., & Nelson, G. (2018). The cross spectrum in multiple input multiple Response vibration testing. *Topics in Modal Analysis & Testing, Volume 9*, 91–102. [https://doi.org/10.1007/978-3-319-74700-2\\_10](https://doi.org/10.1007/978-3-319-74700-2_10).
- Kapp, S., Barz, M., Mukhametov, S., Sonntag, D., & Kuhn, J. (2021). ARETT: Augmented Reality eye Tracking toolkit for head mounted displays. *Sensors*, 21(6), 2234. <https://doi.org/10.3390/s21062234>.
- Kim, J.-I., & Humphreys, G. W. (2010). The Interactive Effects of Colors on Visual Attention and Working Memory: In Case of Images of Tourist Attractions. *Attention, Perception, & Psychophysics*, 72(6), 1533–1555. <https://doi.org/10.3758/app.72.6.1533>.
- Koutitas, G., Smith, S., & Lawrence, G. (2020). Performance evaluation of AR/VR training technologies for EMS First Responders. *Virtual Reality*, 25(1), 83–94. <https://doi.org/10.1007/s10055-020-00436-8>.
- Kuzhagaliyev, T. (2018, May 27). *TCP client in a UWP Unity app on HoloLens*. Foxy Panda. <https://foxypanda.me/tcp-client-in-a-uwp-unity-app-on-hololens/>.
- Linderman, L. E., Mechitov, K. A., & Spencer, B. F. (2012). Tinyos-based real-time wireless data acquisition framework for structural health monitoring and control. *Structural Control and Health Monitoring*, 20(6), 1007–1020. <https://doi.org/10.1002/stc.1514>.

- Loschky, L. C., Nuthmann, A., Fortenbaugh, F. C., & Levi, D. M. (2017). Scene perception from central to peripheral vision. *Journal of Vision*, 17(1), 6. doi:10.1167/17.1.6.
- Lynch J.P., Loh K.J. (2006) A summary review of wireless sensors and sensor networks for structural health monitoring. *Shock Vib Digest* 38(2):91–130.
- Ma, Z., Mei, G., & Piccialli, F. (2021). Machine learning for landslides prevention: a survey. *Neural Computing and Applications*, 33(17), 10881-10907.
- Maeda, Y., Nishiwaki, S., Izui, K., Yoshimura, M., Matsui, K., & Terada, K. (2006). Structural topology optimization of vibrating structures with specified eigenfrequencies and eigenmode shapes. *International Journal for Numerical Methods in Engineering*, 67(5), 597-628.
- Maharjan, D., Aguero, M., Lippitt, C., and Moreu, F. (2019). Infrastructure stakeholders' perspective in development and implementation of new structural health monitoring (SHM) technologies for maintenance and management of transportation infrastructure. *MATEC web of conferences* 271,01010. doi:10.1051/mateconf/201927101010.
- Makarov, A. (2022, April 7). *Augmented reality in retail, marketing, and sales in 2022*. MobiDev. Retrieved from <https://mobidev.biz/blog/augmented-reality-marketing-sales>.
- Manring, L., Pederson, J., Potts, D., Boardman, B., Mascareñas, D., Harden, T., & Cattaneo, A. (2020). Augmented reality for interactive robot control. In *Special Topics in Structural Dynamics & Experimental Techniques, Volume 5* (pp. 11-18). Springer, Cham.
- Mitsushige, O. (1997). Motion control of the satellite mounted robot arm which assures satellite attitude stability. *Acta Astronautica*, 41(11), 739-750.
- Morales Garcia, J.E.; Gertsen, H.J.; Liao, A.S.N.; Mascareñas, D.D.L. *Augmented Reality for Smart Infrastructure Inspection*; Technical report; Los Alamos National Lab. (LANL); Los Alamos, NM, USA, 2017.
- Morimoto, R. (2013). A socio-economic analysis of Smart Infrastructure sensor technology. *Transportation Research Part C: Emerging Technologies*. 31. 18–29. 10.1016/j.trc.2013.02.015.
- Namuduri, S., Narayanan, B. N., Davuluru, V. S. P., Burton, L., & Bhansali, S. (2020). Deep learning methods for sensor based predictive maintenance and future perspectives for electrochemical sensors. *Journal of The Electrochemical Society*, 167(3), 037552.
- Napolitano, R., Liu, Z., Sun, C., & Glisic, B. (2019). Combination of Image-Based Documentation and Augmented Reality for Structural Health Monitoring and Building Pathology. *Frontiers in Built Environment*, 5. doi:10.3389/fbuil.2019.00050.
- Nasimi, R., Moreu, F., Nasimi, M., & Wood, R. (2022). Developing Enhanced Unmanned Aerial Vehicle Sensing System for Practical Bridge Inspections Using Field Experiments. *Transportation Research Record*, 03611981221075618.
- Nasimi, R., Atcitty, S., Thompson, D., Murillo, J., Ball, M., Stormont, J., Moreu, F. (2022). Use of Remote Structural Tap Testing Devices Deployed via Ground Vehicle for Health Monitoring of Transportation Infrastructure. *Sensors*, 22, 1458. <https://doi.org/10.3390/s22041458>.

- Natephra, W. & Motamedi, A. (2019). Live data visualization of IoT sensors using Augmented Reality (AR) and BIM. 10.22260/ISARC2019/0084.
- Opiyo, S., Zhou, J., Mwangi, E. *et al.* A Review on Teleoperation of Mobile Ground Robots: Architecture and Situation Awareness. *Int. J. Control Autom. Syst.* 19, 1384–1407 (2021). <https://doi.org/10.1007/s12555-019-0999-z>.
- Palacios, R.H. (2015). Robotic Arm Manipulation Laboratory With a Six Degree of Freedom JACO Arm. [Thesis]. Naval Postgraduate School.
- Pandey, A. V., Manivannan, A., Nov, O., Satterthwaite, M., & Bertini, E. (2014). The persuasive power of data visualization. *IEEE transactions on visualization and computer graphics*, 20(12), 2211-2220.
- Papakostas, C., Troussas, C., Krouska, A. et al. User acceptance of augmented reality welding simulator in engineering training. *Educ Inf Technol* (2021). <https://doi.org/10.1007/s10639-020-10418-7>.
- Park, H. S., Park, M. W., Wong, K. H., Kim, K., & Jung, S. K. (2013). In-vehicle ar-hud system to provide driving-safety information. *ETRI Journal*, 35(6), 1038-1047. doi:10.4218/etrij.13.2013.0041.
- Porter, M. E., & Heppelmann, J. E. (2017). A Manager's Guide to Augmented Reality. *Harvard Business Review*, 46–57. <https://hbr.org/>.
- Prusaczyk, P., Kaczmarek, W., Panasiuk, J., & Besseghieur, K. (2019). Integration of robotic arm and vision system with processing software using TCP/IP protocol in industrial sorting application. *AIP Conference Proceedings*. <https://doi.org/10.1063/1.5092035>.
- Rosen, E., Whitney, D., Phillips, E., Chien, G., Tompkin, J., Konidaris, G., & Tellex, S. (2019). Communicating and controlling robot arm motion intent through mixed-reality head-mounted displays. *The International Journal of Robotics Research*, 38(12-13), 1513-1526.
- Saadatzi, M., Saadatzi, M. N., Tavaf, V., & Banerjee, S. (2018). "AEVE 3D: Acousto Electrodynamic Three-Dimensional Vibration Exciter for Engineering Testing," in *IEEE/ASME Transactions on Mechatronics*, vol. 23, no. 4, pp. 1897-1906, doi: 10.1109/TMECH.2018.2841011.
- Shin, D. H., and Dunston, P. S. (2008). Identification of application areas for augmented reality in industrial construction based on technology suitability. *Autom. Const.* 17 (7), 882–894. doi:10.1016/j.autcon.2008.02.012.
- Singh, P. K., Kainthola, A., Panthee, S., & Singh, T. N. (2016). Rockfall analysis along transportation corridors in high hill slopes. *Environmental Earth Sciences*, 75(5), 1-11.
- USGS. How Many Deaths Result from Landslides Each Year? 2021. Available online: [https://www.usgs.gov/faqs/how-many-deaths-result-landslides-each-year?qt-news\\_science\\_products=0#qt-news\\_science\\_products](https://www.usgs.gov/faqs/how-many-deaths-result-landslides-each-year?qt-news_science_products=0#qt-news_science_products) (accessed on 16 June 2022).
- Wang, X. (2008). Improving Human-Machine Interfaces for Construction Equipment Operations with Mixed and Augmented Reality. *Robotics and Automation in Construction*. doi:10.5772/5850.
- Webster, A., Feiner, S., MacIntyre, B., Massie, W., and Krueger, T. (1996). Augmented reality in architectural construction, inspection, and renovation. *Proc. ASCE Third Congress on Computing in Civil Engineering* (New York, NY), 913–919.

- Whitney, D., Rosen, E., Ullman, D., Phillips, E., & Tellex, S. (2018, October). Ros reality: A virtual reality framework using consumer-grade hardware for ros-enabled robots. In *2018 IEEE/RSJ International Conference on Intelligent Robots and Systems (IROS)* (pp. 1-9). IEEE.
- Wintersberger, P., Frison, A., Riener, A., & Sawitzky, T. V. (2019). Fostering user acceptance and trust in fully automated vehicles: Evaluating the potential of augmented reality. *PRESENCE: Virtual and Augmented Reality*, 27(1), 46-62. doi:10.1162/pres\_a\_00320.
- Wisanuvej, P., Liu, J., Chen, C. & Yang, G.H. (2014). Blind collision detection and obstacle characterisation using a compliant robotic arm. Proceedings - IEEE International Conference on Robotics and Automation. 2249-2254. 10.1109/ICRA.2014.6907170.
- Xu, J., Wyckoff, E., Hanson, J. W., Moreu, F., & Doyle, D. (2021). Implementing augmented reality technology to measure structural changes across time. *arXiv preprint arXiv:2111.02555*.
- Yang, S., Jung, J., Liu, P., Lim, H. J., Yi, Y., Sohn, H., & Bae, I.-hwan. (2021). Ultrasonic wireless sensor development for online fatigue crack detection and failure warning. *Structural Engineering and Mechanics*, 69(4), 407–416. <https://doi.org/https://doi.org/10.12989/sem.2019.69.4.407>.
- Younis, O., Al-Nuaimy, W., & Rowe, F. (2019). A hazard detection and tracking system for people with peripheral vision loss using smart glasses and augmented reality. *International Journal of Advanced Computer Science and Applications*, 10(2).
- Zhou, X., "Wireless Sensor Network Deployment in Cyberphysical Machine Tool System Based on Optimal Allocation of Memory Buffers", *Journal of Sensors*, vol. 2021, ArticleID 6680718, 18 pages, 2021. <https://doi.org/10.1155/2021/6680718>.
- Zoumpikas, T, Puig, A, Salamó, M, García-Sellés, D, Blanco Nuñez, L, Guinau, M. An intelligent framework for end-to-end rockfall detection. *Int J Intell Syst.* 2021; 36: 6471- 6502. <https://doi.org/10.1002/int.22557>.